European Journal of Life Sciences

Volume: 3 • Issue: 3 • December 2024 • ISSN: 2822-5333

ANADOLU UNIVERSITY
Faculty of Pharmacy

ANADOLU UNIVERSITY
Faculty of Pharmacy

European Journal of Life Sciences

Volume: 3 • Issue: 3 • December 2024

ISSN: 2822-5333

European Journal of Life Sciences

Owner of the Journal on behalf of Anadolu University
Prof. Dr. Yusuf Adıgüzel

Editor in Chief
Prof. Dr. Gülşen Akalın Çiftçi

Editors
Prof. Dr. Mehlika Dilek Altıntop
Assoc. Prof. Dr. Hale Gamze Ağalar

Publication Type
International peer-reviewed journal

Publication Frequency
Triannually

Language
English

Website
https://dergipark.org.tr/ejls

Publisher
Anadolu University Faculty of Pharmacy

Publisher Address
Anadolu University, Faculty of Pharmacy
Yunus Emre Campus, 26470 Tepebaşı/Eskişehir
Phone: +90 222 335 05 80
E-mail: ejls@anadolu.edu.tr
Web: https://eczacilik.anadolu.edu.tr

Publishing Services
Akdema Informatics, Publishing, and Consultancy Trade LLC
Address: Kızılay Mahallesi, Gazi Mustafa Kemal Bulvarı No: 23/8, 06420 Çankaya/Ankara
E-mail: bilgi@akdema.com
Phone: +90 533 166 80 80
Web site: www.akdema.com

European Journal of Life Sciences

Editorial Board

European Journal of Life Sciences

Contents

ANADOLU UNIVERSITY
FACULTY OF PHARMACY

European Journal of Life Sciences 2024; 3: 93-100

Research Article

Quantitative determination of rivaroxaban in pharmaceutical formulations by ultra performance liquid chromatography

Murat Kozanlı[1,2], Nafiz Öncü Can[2,3]

[1]Bilecik Şeyh Edebali University, Health Services Vocational School, Pharmacy Services, Bilecik, Türkiye.
[2]Anadolu University, Faculty of Pharmacy, Central Research Laboratory, Eskişehir, Türkiye.
[3]Anadolu University, Faculty of Pharmacy, Department of Analytical Chemistry, Eskişehir, Türkiye.

✉ Murat Kozanlı
murat.kozanli@bilecik.edu.tr

https://doi.org/10.55971/EJLS.1535613

Received: 19.08.2024
Accepted: 16.12.2024
Available online: 31.12.2024

ABSTRACT

Rivaroxaban, which is a factor Xa inhibitor, effectively prevents clot formation in cardiovasculary system. In this study, a novel UPLC method was developed to provide an accurate, sensitive, fast, and reliable way for qualitative and quantitative analysis of rivaroxaban in pharmaceutical dosage forms. Chromatographic separation was achieved using a Phenomenex C18-bonded fused-core silica column (Kinetex® 2.6 µm, 150 mm × 3 mm i.d.). The separation was performed in isocratic mode with a mobile phase consisting of water, acetonitrile, and methanol (55:20:25, *v/v/v*), at a flow rate of 0.5 mL min^{-1}, a column temperature of 40 °C, and a detection wavelength of 249 nm. The method was validated according to ICH Q2(R1) guideline for linearity, range, LOD and LOQ, accuracy, and precision and was successfully implemented to the analysis of rivaroxaban in tablet formulations.

Keywords: Rivaroxaban, Pharmaceutical formulation, UPLC

1. INTRODUCTION

Rivaroxaban (RIV) is an oral anticoagulant used to prevent blood clots, belonging to the oxazolidinone family. It is a potent selective inhibitor of factor Xa, effectively preventing venous thromboembolism in people who have undergone surgery [1,2]. It has high oral bioavailability, predictable pharmacokinetics, a rapid onset of action and strong effect [3]. RIV is clinically effective in the treatment of thromboembolism [4]. RIV is a blood thinner with a molecular formula $C_{19}H_{18}ClN_3O_5S$ and molecular weight 435.882 g mol^{-1} (Figure 1). It has low solubility in organic solvents and is virtually insoluble in water and aqueous media. log P for RIV is 1.74-1.9 with pKa 13.6 (most acidic) and 1.6 (most basic) [5,6].

HPLC is a crucial technique for analysis of pharmaceutical raw materials, by-products, formulations and finished products, in all steps of pharmaceutical production. Advances in the column technology, which is the heart of the technique, provide enhanced chromatographic performance with better limits, analysis performance and peak shapes [7]. In accordance, HPLC seem to remain as the gold-technique in drug analysis, especially for analysis of non-volatile compounds. The ultra performance liquid chromatography method (UPLC), which is evolved from HPLC, is a completely faster

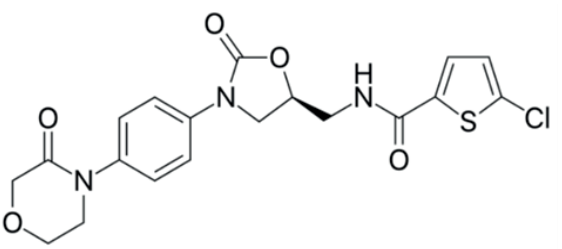

Figure 1. Molecular structure of RIV

system with advanced technology in instrumental components, such as pumps, detectors, autosamplers, etc. This means shorter analysis time, less solvent consumption and higher throughput [8]. UV-Visible Spectrophotometry [9-15], HPLC [2, 16-26], UPLC [27, 28], HPTLC [29, 30] and LC-MS [31, 32] have been published for RIV analysis in pharmaceutical formulations. The fact that UPLC analysis for RIV determination is less common than other ways of analysis has led us to appraise our study into use of different stationary phases and contents. In pharmaceutical field, there is always a need for fast, simple, accurate and sensitive analysis methods. Thus, we developed a simple and rapid UPLC method for the determination of RIV in pharmaceutical tablet formulations. This method addresses the limitations of existing analytical techniques by offering enhanced sensitivity, improved reliability, and greater practicality. Following comprehensive optimization and validation including assessments of accuracy, precision, and linearity the proposed method has proven suitable for quality control of RIV tablets.

2. MATERIALS AND METHODS

2.1. Chemical and Reagents

RIV reference standard with min 99.5% (*w/w*) purity from Molekula (USA) and Escitalopram (ESC, as internal standard) from United States Pharmacopeial Convention (USA) were purchased. Analytical grade chemicals; HPLC gradient grade acetonitrile (ACN), methanol (MeOH) and water for chromatography were obtained from Sigma-Aldrich (Germany).

2.2. Instruments

Analyses were performed using a Shimadzu Nexera-i 2040C 3D series compact ultra performance liquid chromatography system (Japan); chromatograms were processed by using Shimadzu LabSolution Version 5.81 data analysis software.

2.3. Chromatographic Parameters

The mobile phase was composed of water: ACN:MeOH in the ratio of 55:20:25, *v/v/v*. Chromatographic separation was performed using a C18-bonded core shell silica column (Phenomenex Kinetex® 2.6 µm, 150 mm × 3 mm inner diameter). The column oven temperature was set at 40 °C. Samples were injected at 10 µL aliquotes, and flow rate was applied as 0.5 mL/min. To determine the optimal wavelength for analysis, spectra were recorded across a range of 200 to 800 nm. As a result, the maximum absorbance of RIV was determined by UV-Visible Spectroscopy at a wavelength of 249 nm as shown in Figure 2.

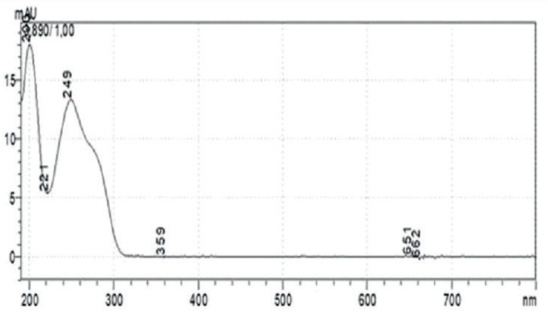

Figure 2. Maximum absorption spectrum of RIV with UV-Visible Spectroscopy

2.4. Preparation of Solutions

MeOH:water (40:60, *v/v*) (dilution mixture) solution was used for all dissolution/dilution procedures. For the preparation of the stock solution I, exactly-weighed 5 mg of RIV was taken and dissolved in dilution mixture in a 10 mL volumetric flask, by mixing with a stirrer for 3 minutes to ensure dissolution. As an intermediate, stock solution II at 100 µg mL^{-1} concentration was prepared by dilution of the stock solution I; stock solution II was used to quantify RIV in both samples and test solutions. ESC was used as internal standart at 50 µg mL^{-1} concentration. An amount of powdered tablets equal to the average tablet weight was also dissolved in 100 mL of the dilution mixture. Resulting mixture was centrifuged at 4000 rpm for 10 min. The supernatant was filtered through a 0.22 µm pore diameter PVDF filter.

2.5. Validation of Analytical Method

2.5.1. Testing of System Suitability

System suitability was recognized as the appropriateness of the instrumentation to analytical quantification requirements. Calculations for

capacity factor (k), tailing factor (T), resolution (Rs), and theoretical number of plates (N) was performed according to United States Pharmacopoeia (USP).

2.5.2. Specificity

In accordance with the ICH Q2(R1) guideline, additional examinations were conducted to evaluate method specificity [33]. Chromatograms and peaks were carefully analyzed to ensure that there was no interference, false peaks, or unexpected signals that could affect the accuracy of the analysis. Peak purity was assessed to ensure that the observed peaks for both the analyte and the internal standard were not the result of co-elution with other compounds. This evaluation confirmed that the detected peaks correspond exclusively to their respective compounds.

2.5.3. Linearity and Range

Seven different levels (9.98, 20, 40, 50, 60, 80 and 99.8 µg/mL) of RIV concentrations were included in a linearity range. Each solution was injected as three times, and the average values were used for further quality control calculations. Linear regression, including both intra-day and inter-day repeats, was used to assess linearity. All statistical calculations were made with GraphPad Prism v6.0b (trial).

2.5.4. Precision

The precision of an analytical method is a measure of the consistency and reproducibility of the results obtained from multiple measurements of the same sample under specified conditions. Reproducibility results are given as standard deviation and relative standard deviation to describe the precision of the method.

2.5.5. Accuracy

Accuracy refers to how the measured values are coles to the accepted reference value. It reflects the extent of any systematic error or bias introduced by the analytical method. In practical terms, accuracy is often assessed through recovery experiments. These involve adding known quantities of the active compounds (analytes) to real sample matrices and measuring how much of the added amount can be recovered. The results are expressed as a percentage of recovery, providing a quantitative measure of the method's accuracy.

2.5.6. Limitations of Detection and Quantification

According to the guidelines established by the International Council for Harmonization of Technical Requirements for Pharmaceuticals for Human Use (ICH), the LOD and LOQ values were determined based on the standard deviation of the response and the slope of the calibration curve. The detection limit was determined as the concentration corresponding to 3.3 times the signal-to-noise ratio. For the quantification limit, a concentration equivalent to 10 times the noise level was prepared and analyzed in 10 replicates to ensure accuracy and precision.

3. RESULTS AND DISCUSSION

The reported method has been examined and verified with the parameters of system conformity tests, linearity, selectivity, LOD and LOQ, precision and accuracy specified in the guidelines of the International Conference on Harmonization (ICH Q2(R1)). System Suitability Testing (SST) is an important part of analytical method development and validation. It is necessary to determine the most suitable conditions for a good separation of the desired analytes in the analyzes. In determining the most suitable conditions, analyses were conducted to optimize factors such as the mobile phase composition, flow rate, analytical columns, column temperature, detector wavelength, and injection volume. In determining the mobile phase content, it is necessary to provide short elution time and good peak symmetry. In the selection of the mobile phase to be used in the optimization process, analyzes were tried at different rates with water-ACN and water-MeOH mixtures at the beginning. Then, analyses were performed with different ratios of water, MeOH and ACN solvents and the most suitable environment was provided with water:ACN:MeOH (55:20:25, *v/v/v*) mobile phase composition. To determine the mobile phase flow, analyses were performed between 0.3 and 1.0 mL min^{-1}. For the best separation and short analysis time, 0.5 mL min^{-1} was found to appropriate. The result of column temperature variation on the analysis was

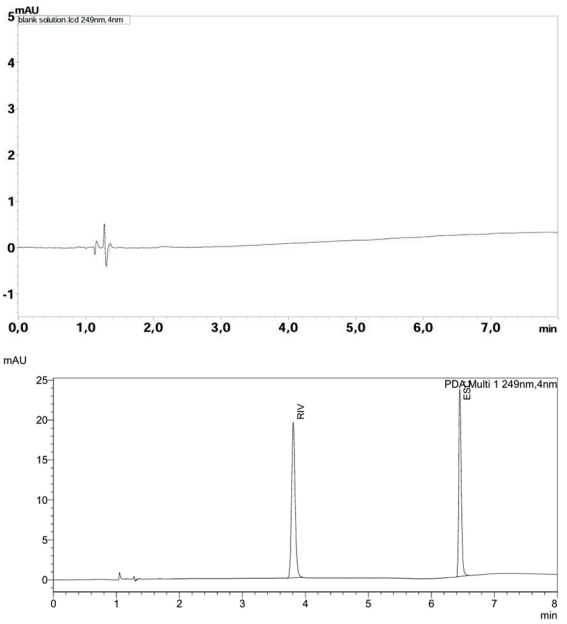

Figure 3. The chromatogram of blank solution and standard solutions (10 µg mL^{-1} for RIV, 50 µg mL^{-1} for ESC)

investigated at temperatures of 25, 30, 40, and 50 °C. It is determined as an operating temperature of 40 °C under optimum conditions. In the preliminary studies carried out with UV-Spectroscopy and UPLC-DAD detector for the determination of the study wavelength, the wavelength that creates a response in accordance with the chemical structure of the substance was determined as 249 nm. With its high absorbance, a wavelength of 200 nm could also be selected for analysis. But it was not chosen because there would be a high fluctuation in the mobile phase line. During the optimization studies, 10 µg mL^{-1} RIV and 50 µg mL^{-1} standard substances were used and the chromatogram is given in Figure 3. The mobile phase flow rate was set to 0.5 mL min^{-1} to achieve low system pressure and optimal elution time.

In addition, the system suitability parameters for the developed method are summarized in Table 1. As a result of the optimised conditions according to USP Pharmacopoeia very suitable results were obtained according to the recommended values.

Linearity was demonstrated at seven different concentrations in the range of 9.98-99.8 µg mL^{-1}. Injection of each solution was carried out in triplicate and linearity was plotted with the mean values obtained. Linearity results were found as slope, intercept, and correlation coefficient as shown in Table 2. The method showed good linearity as 0.9999. LOD and LOQ of the assay were calculated as the ratio of the standard deviation (σ) of the response to the slope (m) of the calibration curve 3.3 and 10. The values of LOD and LOQ for RIV were found to be 1.22 and 3.70, respectively. Recovery studies were carried out with XARELTO®, which contains the active ingredient RIV, which is available in the market. First of all, the RIV standard substance was added to the prepared test solutions with certain quantities. The analyses were carried out at three different concentrations and nine different analyses.

Table 1. System suitability results (n=3)

Parameter	RIV	ESC	Recommended value (USP)
Retention Time (minute)	3.85	6.40	-
Tailing Factor (*T*)	1.2	1.9	0.1<T≤ 1.8
Capacity Factor (*k*)	2.2	4.2	2<k<10
Resolution (R_s)	20.5	27.2	Rs>1.5
Number of theoretical plate (*N*)	19600	12200	N>2000
Repeatability of peak area (*%RSD*)	0.94	0.68	%RSD < 1.0

Table 2. Results of validation studies performed to evaluate method linearity, LOD, LOQ for RIV (n=7)

Parameter	Calculated value
Linearity range (µg mL^{-1})	9.98 - 99.8
Slope±SD (n=7)	5837 ± 117.2
Intercept ±SD (n=7)	1567 ± 24
R^2 (n=7)	0.9999
Limit of detection (S/N=3.3, µg mL^{-1})	1.22
Limit of quantitation (S/N=10, µg mL^{-1})	3.70

Table 3. Accuracy and precision data of RIV

Spiked concentration (µg mL^{-1})	Obtained concentration (µg mL^{-1})± SD; %RSD	Recovery (%)	Bias (%)	Intra-day precision (n = 4) Mean concentration (µg mL^{-1}) ± SD; %RSD	Inter-day precision (n = 4) Mean concentration (µg mL^{-1}) ± SD; %RSD
40	40.41±0.57; 1.41	101.03	1.03	40.05±0.11; 0.28	40.30±0.71; 1.76
50	50.16±0.30; 0.60	100.32	0.32	50.44±0.80; 1.58	49.97±0.28; 0.56
60	59.47±0.67; 1.12	99.12	0.88	60.25±0.78; 1.29	60.47±0.69; 1.15

As a result of the analysis, the results were obtained as given in Table 3.

The developed method demonstrated high precision and accuracy, as shown by intra-day and inter-day analyses of standard RIV solutions at concentrations of 40.0, 50.0, and 60.0 µg mL^{-1}. Precision was confirmed by RSD% values consistently below 2.0, and accuracy was validated with Bias% values also under 2.0. These results highlight the method's reliability and robustness.

Tablet Assay

Tablet samples (XARELTO 10 mg and 20 mg 28 tablet) obtained from BAYER TURK were subjected to analysis to test the applicability of proposed method and to specify rivaroxaban content. Recovery tests were conducted using the conventional addition procedure, with a total of nine independent determinations performed at three different concentrations within the target range. Recovery studies were carried out by adding a certain amount of standard solution mixture while preparing the tablet solutions. In Table 4 and Figure 4 results and values were found to be in accordance with official regulations.

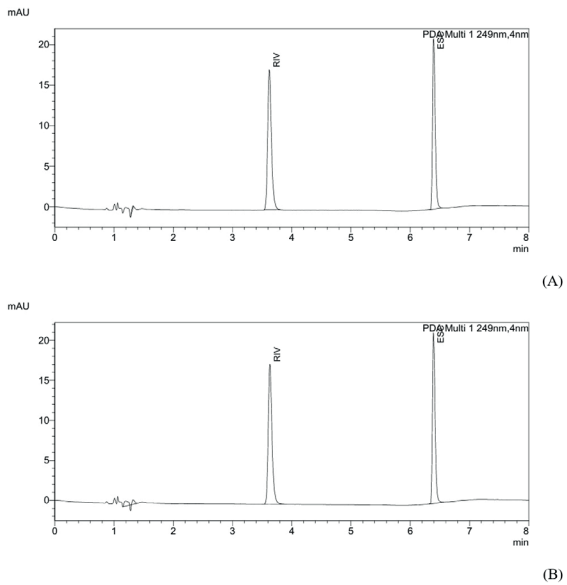

Figure 4. Chromatograms of 10 mg (A) and 20 mg (B) tablet solutions

Table 4. RIV assay in tablets (XARELTO® 10 mg and 20 mg)

Labeled drug claim in tablet (mg)	Determined content of drug (mg)	SD	RSD (%)	Recovery (%)
10	9.98	0.03	0.32	99.80
20	20.02	0.07	0.32	100.10

Results of the determination of RIV in pharmaceutical tablet formulations are shown in Table 4. The accuracies of the UPLC method for 10 mg and 20 mg were 99.80% and 101.10%, respectively, confirming the accuracy of the proposed methods.

4. CONCLUSION

This study developed and validated a rapid, accurate, and precise UPLC method for the qualitative and quantitative analysis of rivaroxaban in pharmaceutical preparations. A simple sample preparation and a short chromatographic study time were used.

Due to the hybrid of the liquid chromatography device used in the developed method, it is advantageous both in terms of working at high pressures and using larger diameter columns compared to other UPLC devices. In this way, analysis is carried out in a short time and allows less consumption of the chemicals used.

The linearity test results show that there is a good correlation between $R \geq 0.9999$ and the peak area and concentration for rivaroxaban and that the calibration curve is method linear over the studied concentration range. In addition, reproducibility and accuracy criteria are provided. The low retention time and the values of the detection limit (1.22 µg mL^{-1}) and quantification limits (3.70 µg mL^{-1}) show the superiority of the method over other methods.

The proposed liquid chromatography method stands out with its speed, simplicity, use of environmentally friendly solvents and low solvent consumption compared to similar studies in the literature. These features make the method more reliable and sustainable. For these reasons, the proposed method will greatly simplify the work of analysts in quality control laboratories, particularly for the analysis of formulations and finished products. It will also provide information for advanced analysis methods related to RIV.

Ethical approval

Not applicable, because this article does not contain any studies with human or animal subjects.

Author contribution

Conceptualization, M.K. and N.Ö.C.; Methodology, M.K. and N.Ö.C.; Software, M.K.; Validation, M.K. and N.Ö.C.; Formal analysis, M.K. and N.Ö.C.; Investigation, M.K.; Resources, M.K.; Data curation, N.Ö.C.; Writing—original draft preparation, M.K. and N.Ö.C.; Writing—review and editing, M.K.; Visualization, M.K. and N.Ö.C.; Supervision, N.Ö.C.; Project administration, N.Ö.C.; Funding acquisition, N.Ö.C. All authors have read and agreed to the published version of the manuscript.

Source of funding

This research received no grant from any funding agency/sector.

Conflict of interest

The authors declared that there is no conflict of interest.

REFERENCES

1. Eswarudu M, Devi AL, Pallavi K, Babu PS, Priya SN, Sulthana SHS. Novel validated RPHPLC method for determination of rivaroxaban in bulk and its pharmaceutical dosage form. Int J Pharm Sci Rev Res. (2020);64(1):183-187. https://doi.org/10.47583/ijpsrr.2020.v64i01.033
2. Çelebier M, Reçber T, Koçak E, Altinöz S. RP-HPLC method development and validation for estimation of rivaroxaban in pharmaceutical dosage forms. Braz J Pharm Sci. (2013); 49:359-366. https://doi.org/10.1590/S19848250201300020018
3. Perzborn E, Roehrig S, Straub A, Kubitza D, Misselwitz F. The discovery and development of rivaroxaban, an oral, direct factor Xa inhibitor. Nat Rev Drug Discov. (2011);10(1):61-75. https://doi.org/10.1038/nrd3185
4. Vanassche T, Vandenbriele C, Peerlinck K, Verhamme P. Pharmacotherapy with oral Xa inhibitors for venous thromboembolism. Expert Opin Pharmacother. (2015);16(5):645-658. https://doi.org/10.1517/14656566.2015.999043
5. Reçber T, Haznedaroğlu İC, Çelebier M. Review on characteristics and analytical methods of rivaroxaban. Crit Rev Anal Chem. (2022);52(4):865-877. https://doi.org/10.1080/10408347.2020.1839735
6. Samama MM. The mechanism of action of rivaroxaban–an oral, direct Factor Xa inhibitor– compared with other anticoagulants. Thromb Res. (2011);127(6):497-504. https://doi.org/10.1016/j.thromres.2010.09.008
7. Özcan S, Öğüt EG, Levent S, Can NÖ. A new HPLC method for selexipag analysis in pharmaceutical formulation and bulk form. Eur J Health Sci. (2023);2(2):53-58. https://doi.org/10.55971/EJLS.1320502
8. Gumustas M, Kurbanoglu S, Uslu B, Ozkan SA. UPLC versus HPLC on drug analysis: advantageous, applications and their validation parameters. Chromatographia. (2013);76:1365-1427. https://doi.org/10.1007/s10337-013-2477-8
9. Bhavyasri K, Dhanalakshmi C, Sumakanth M. Development and validation of ultra violetvisible spectrophotometric method for estimation of rivaroxaban in spiked human plasma. J Pharm Sci Res. (2020);12(9):1215-1219.
10. Çelebier M, Kaynak M, Altınöz S, Şahin S. UV spectrophotometric method for determination of the dissolution profile of rivaroxaban. Dissolution Technol. (2014);21(4):56-59. https://doi.org/10.14227/DT210414P56
11. Sekaran CB, Bind VH, Damayanthi MR, Sireesha A. Development and validation of UV spectrophotometric method for the determination of rivaroxaban. Der Pharma Chemica. (2013);5(4):1-5.
12. Pinaz AK, Muralikrishna K. Area Under Curve Spectrophotometric Method for Determination of Rivaroxaban in Bulk and Tablet Formulation and Its Validation. Asian J Pharm Res. (2013);3(3):109-113.
13. Seshamamba B, Sekaran C. Spectrophotometric quantification of direct factor xa inhibitor, rivaroxaban, in raw and tablet dosage form. Glob Drugs and Therap. (2017);2(3):1-8. https://doi.org/10.15761/GDT.1000122
14. Seshamamba BSV, Sekaran CB. Spectrophotometric Analysis for the Quantification of Rivaroxaban in Bulk and Tablet Dosage Form. Int J Med Pharm Sci. (2017);7:21-34.
15. El-Bagary RI, Elkady EF, Farid NA, Youssef NF. A Validated Spectrophotometric Method and Thermodynamic Studies for the Determination of Cilostazol and Rivaroxaban in Pharmaceutical Preparations Using Fe-Phenanthroline System. Anal Chem Lett. (2017);7(5):676-688. https://doi.org/10.1080/22297928.2017.1385420
16. Sahoo S, Mekap SK. Assay comparison of rivaroxaban by new HPLC method with an existing method in tablet dosage form. Pharm Biol Eval. (2017);4:180-182. https://doi.org/10.26510/2394-0859.pbe.2017.27
17. Nımje H, Chavan R, Pawar S, Deodhar M. Development and validation of stabilityindicating RP-HPLC method for rivaroxaban in tablet dosage form. J Res Pharm. (2022);26(6):1703-1712. https://doi.org/10.29228/jrp.261
18. Kasad PA, Muralikrishna K. Design and validation of dissolution profile of rivaroxaban by using RP-HPLC method in dosage form. Asian J Pharm Anal. (2013);3(3):75-78.
19. Pinaz AK, Muralikrishna K. Method development and acid degradation study of rivaroxaban by RP-HPLC in bulk. Asian J Pharm Anal. (2013);3(2):62-65.
20. Lories I, Mostafa A, Girges M. High performance liquid chromatography, TLC densitometry, first derivative and first derivative ratio spectrophotometry for determination of rivaroxaban and its alkaline degradates in bulk powder and its tablets. J Chromatogr Sep Tech. (2013);4(8):1-6. https://doi.org/10.4172/2157-7064.1000202
21. Seshamamba BSV, Satyanarayana PVV, Sekaran CB. Application of stability indicating HPLC method with UV detector to the analysis of rivaroxaban in bulk and tablet dosage form. Chem Sci Trans. (2014);3(4):1546-1554. https://doi.org/10.7598/cst2014.893
22. Walter ME, Perobelli RF, Da Silva FS, Cardoso Junior C, da Silva IS, Dalmora SL. Development and validation of a stability-indicating RP-HPLC method for the determination of rivaroxaban in pharmaceutical formulations. Lat American J Pharm. (2015);34(8):1503-1510.

23. Hadagali MD. Determination of rivaroxaban in pure, pharmaceutical formulations and human plasma samples by RP-HPLC. Int J Adv Pharm Anal. (2015);5(3):65-68. https://doi.org/10.7439/ijapa.v5i3.2800

24. Souri E, Mottaghi S, Zargarpoor M, Ahmadkhaniha R, Jalalizadeh H. Development of a stability-indicating HPLC method and a dissolution test for rivaroxaban dosage forms. Acta Chromatogr. (2016);28(3):347-361. https://doi.org/10.1556/1326.2016.28.3.05

25. Girase Y, Srinivasrao V, Soni D. Development and validation of stability-indicating RPHPLC method for rivaroxaban and its impurities. SOJ Biochem. (2018);4:1-6. https://doi.org/10.15226/2376-4589/4/1/00127

26. Badroon T, Sreeramulu J. Development and validation of stability indicating assay by HPLC method for estimation of Rivaroxaban. Int J Bio-Pharm Res. (2019);8(5):2582-2586.

27. Rajan N, Basha KA. A stability-indicating ultra-performance liquid chromatographic method for estimation of related substances and degradants in Rivaroxaban active pharmaceutical ingredient. J Pharm Res. (2014); 8(11):1719-1725.

28. Rao P, Cholleti V, Reddy V. Stability-indicating UPLC method for determining related substances and degradants in Rivaroxaban. Int J Res Pharm Sci. (2015); 5(2):17-24.

29. Vaghela D, Patel P. High performance thin layer chromatographic method with densitometry analysis for determination of rivaroxaban from its tablet dosage form. International Int J Pharm Pharm Sci. (2014);6(6):383-386.

30. Alam P, Ezzeldin E, Iqbal M, Anwer MK, Mostafa GA, Alqarni MH, Foudah AI, Shakeel F. Ecofriendly densitometric RP-HPTLC method for determination of rivaroxaban in nanoparticle formulations using green solvents. RSC Advances. (2020);10(4):2133-2140. https://doi.org/10.1039/C9RA07825H

31. Ramisetti NR, Kuntamukkala R. Development and validation of a stability indicating LCPDA-MS/MS method for separation, identification and characterization of process related and stress degradation products of rivaroxaban. RSC Advances. (2014);4(44):23155-23167. https://doi.org/10.1039/C4RA00744A

32. Arous B, Al-Mardini MA, Ghazal H, Al-Lahham F. Stability-Indicating Method for the Determination of Rivaroxaban and its Degradation Products using LC-MS and TLC. Res J Pharm Technol. (2018);11(1):212-220. https://doi.org/10.5958/0974-360X.2018.00040.9

33. Borman P, Elder D. Q2 (R1) validation of analytical procedures: text and methodology. ICH quality guidelines: an implementation guide; (2017).p.127-166. https://doi.org/10.1002/9781118971147.ch5

ANADOLU UNIVERSITY
FACULTY OF PHARMACY

European Journal of Life Sciences 2024; 3: 101-106

Research Article

Synthesis of novel thiazole derivatives against Alzheimer's disease and investigation of their cholinesterase inhibition and antioxidant properties

Abdüllatif Karakaya[1,2], Tuğba Erçetin[3], Ulviye Acar Çevik[4], Yusuf Özkay[4]

[1]Anadolu University, Graduate School, Eskişehir, Türkiye.

[2]Zonguldak Bülent Ecevit University, Faculty of Pharmacy, Department of Pharmaceutical Chemistry, Zonguldak, Türkiye.

[3]Eastern Mediterranean University, Faculty of Pharmacy, Department of Pharmacognosy, Gazimagusa, Cyprus.

[4]Anadolu University, Faculty of Pharmacy, Department of Pharmaceutical Chemistry, Eskişehir, Türkiye.

✉ Abdüllatif Karakaya
a.karakaya@beun.edu.tr

https://doi.org/10.55971/EJLS.1585832

Received: 15.11.2024
Accepted: 13.12.2024
Available online: 31.12.2024

ABSTRACT

In this study, 7 new thiazole derivatives were synthesized. Cholinesterase inhibition and antioxidant properties were examined to understand whether the synthesized compounds were anti-Alzheimer drug candidates. The antioxidant properties of these newly synthesized thiazole derivatives and their enzyme inhibition values for acetylcholinesterase (AChE) and butyrylcholinesterase (BuChE) were evaluated. According to the data, these substances inhibited the AChE and BuChE enzymes at deficient levels. Compound **2e** showed the highest AChE inhibition effect with a value of 20.32 ± 0.005% at 50 µM concentration. Although high activity against BuChE was not observed, compound **2d** was an exception with a value of 32.54 ± 0.021% at 50 µM concentration. Values that were comparable to the reference medication gallic acid were found when the antioxidant qualities were investigated using DPPH and ferric ion chelation studies. Ferrous ion-chelating and DPPH radical scavenging consistent with all of the previously reported information, the compounds' antioxidant properties were very high, despite their modest cholinesterase enzyme inhibitory capabilities. In terms of AChE inhibition and antioxidant activity, respectively, compounds **2e** and **2f** were shown to be promising prospective agents among these compounds'.

Keywords: AChE, BuChE, Antioxidant, Thiazole

1. INTRODUCTION

Alzheimer's Disease (AD) is one of the most common diseases among older people. It was first reported in 1906, and information about the progression of the disease was given [1]. AD is the leading cause of dementia worldwide. Characterized by neurodegenerative disorders of the brain, the disease has a prevalence of more than 10,000 per million people and continues to increase with the increasing elderly population. Globally, dementia is causing a major public health crisis. AD accounts for 70% of all dementia cases. It is a disease characterized by neuropathological events such as neuronal cell loss, amyloid β peptide (Aβ) accumulation in extracellular plaques, and intracellular tau (τ) protein accumulation [2]. The amyloid cascade theory of Aβ deposition is a widely recognised hypothesis that posits a causal relationship between the accumulation of Aβ peptides in the brain and the development of AD [3]. There is no problem with the production and

metabolism of Aβ in healthy individuals. However, in the case of AD, this process is disrupted and Aβ accumulates between neuronal cells. Consequently, due to this accumulation, disturbances in nerve conduction, decline in cognitive activities and memory loss occur [4]. The dementia formation pathway is shown in Figure 1.

The etiopathogenesis of the disease is not entirely explained by the Aβ hypothesis. In this case, neurodegeneration is caused by the τ protein, which manifests as a secondary pathogenic event. In neuronal cells, Aβ causes τ protein changes. This protein is primarily responsible for maintaining microtubule stability, undergoes hyperphosphorylation in the case of AD, and hyperphosphorylated protein structures accumulate in neuronal regions and lose their functions. As a result, disruptions in axon transmission are observed [5]. In addition to the pathophysiological events mentioned above, AD is also related to the dysregulation in the cholinergic system. The cholinergic hypothesis has been put forward to explain these dysregulations. This hypothesis is one of the most basic approaches accepted for the treatment of AD [6]. Acetylcholine (ACh) is found in many regions of the brain and plays a role in many events such as learning, memory, stress management, and regulation of cognitive functions [7]. ACh is found in important brain regions

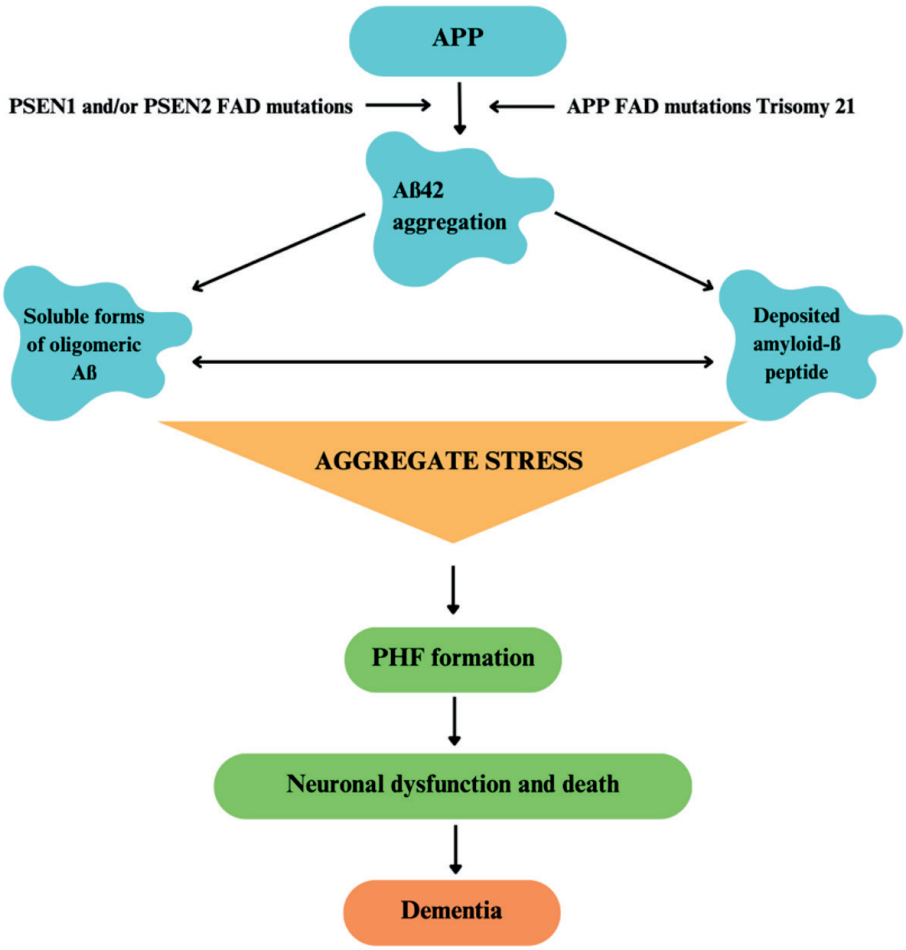

Figure 1. Mutations in presenilin 1 (PSEN1), presenilin-2 and amyloid precursor protein (APP) genes are the main genetic causes of AD. The concept of Aβ derived soluble ligands or soluble toxic oligomers has been proposed to explain the neurotoxicity of Aβ peptide. We would prefer to refer to this as "aggregate stress" in order to highlight potential mechanisms that may result in the formation of paired helical filaments (PHFs) of τ protein aggregates, Aβ aggregation, and ultimately neuronal loss because the mechanisms of action of these species are not fully understood [3].

such as the basal forebrain, cerebral neocortex and hippocampus. It is degraded by the enzyme acetylcholinesterase (AChE) to choline and acetate [8]. In order to normalize the decreasing ACh levels in the later stages of the disease, the basic approach followed in the treatment is to suppress the enzymes AChE, which breaks down the neurotransmitter, and butyrylcholinesterase (BuChE), which is activated when AChE cannot fulfill its function [9].

In this study, thiazole derivatives were synthesized and their structure was clarified using HRMS, ^{1}H-NMR, and ^{13}C-NMR. Ferrous ion-chelating and DPPH radical scavenging methods were used to evaluate the compounds' antioxidant qualities. Additionally, this study aimed at these derivatives' ability to inhibit AChE and BuChE *in vitro*.

2. MATERIALS AND METHODS

2.1. Chemistry

Synthesis of (*E*)-2-((1-methyl-1*H*-pyrrol-2-yl) methylene)hydrazine-1-carbothioamide (1): Ethanol solvent was employed to dissolve 1-methyl-1*H*-pyrrole-2-carbaldehyde and thiosemicarbazide. Three hours were spent refluxing the resultant mixture. After the reaction was finished, the resultant solution was placed in a bath of ice to chill. Filtration was then used to isolate the resultant precipitate.

Synthesis of Target Compounds (2a-2g): Ethanol was utilized to dissolve Compound 1 and a derivative of 2-bromoacetophenone. Four hours were spent refluxing the resultant mixture. Following the completion of the reaction, the mixture was transferred to an ice bath to cool. The precipitate that is produced was isolated by filtration. Subsequently, the precipitate was dried and crystallized by ethanol.

4-(4-Cyanophenyl)-2-(2-((1-methylpyrrol-2-yl) methylene)hydrazineyl)thiazole (2a): Yield: 78 %, M.P.= 195.0 °C. ^{1}H-NMR (400 MHz, DMSO-d_6): δ: 3.86 (3H, s, CH_3), 6.08 (1H, s, Aromatic CH), 6.42 (1H, s, Aromatic CH), 6.95 (1H, s, Aromatic CH), 7.59 (1H, s, Aromatic CH), 7.86 (2H, d, *J*=7.84 Hz, 1,4-disubstituted benzene), 7.99 (1H, s, CH=N), 8.02 (2H, d, *J*=7.40 Hz, 1,4-disubstituted benzene), 11.91 (1H, s, NH). ^{13}C-NMR (100 MHz, DMSO-d_6): δ= 36.92 (CH_3), 107.40, 108.52, 109.97, 114.71, 119.47, 126.56, 127.39, 128.31, 133.13, 136.26, 139.28, 149.22, 169.20. HRMS (*m/z*): $[M+H]^+$ calcd for $C_{16}H_{13}N_5S$: 308.0964; found: 308.0966.

4-([1,1'-biphenyl]-4-yl)-2-(2-((1-methylpyrrol-2-yl)methylene)hydrazineyl)thiazole (2b): Yield: 79 %, M.P.= 220.7 °C. ^{1}H-NMR (400 MHz, DMSO-d_6): δ: 3.88 (3H, s, CH_3), 6.09 (1H, s, Aromatic CH), 6.42 (1H, s, Aromatic CH), 6.95 (1H, s, Aromatic CH), 7.34 (1H, s, Aromatic CH), 7.38 (1H, d, *J*=6.92 Hz, Aromatic CH), 7.48 (2H, t, *J*=6.72 Hz, Aromatic CH), 7.72 (4H, d, *J*=7.48 Hz, Aromatic CH), 7.94 (2H, d, *J*=7.64 Hz, Aromatic CH), 7.99 (1H, s, CH=N), 11.84 (1H, s, NH). ^{13}C-NMR (100 MHz, DMSO-d_6): δ= 36.93 (CH_3), 103.07, 108.48, 114.49, 119.28, 120.70, 126.53, 126.93, 127.28, 127.52, 127.92, 128.17, 129.43, 135.92, 139.44, 140.14, 168.95. HRMS (*m/z*): $[M+H]^+$ calcd for $C_{21}H_{18}N_4S$: 359.1325; found: 359.1336.

4-(3,4-Dichlorophenyl)-2-(2-((1-methylpyrrol-2-yl)methylene)hydrazineyl)thiazole (2c): Yield: 69 %, M.P.= 198.5 °C. ^{1}H-NMR (400 MHz, DMSO-d_6): δ: 3.86 (3H, s, CH_3), 6.09 (1H, s, Aromatic CH), 6.42 (1H, s, Aromatic CH), 6.95 (1H, s, Aromatic CH), 7.50 (1H, s, Aromatic CH), 7.66 (1H, d, *J*=8.32 Hz, Aromatic CH), 7.83 (1H, d, *J*=8.32 Hz, Aromatic CH), 7.97 (1H, s, CH=N), 8.07 (1H, s, Aromatic CH), 11.86 (1H, s, NH). ^{13}C-NMR (100 MHz, DMSO-d_6): δ= 36.94 (CH_3), 107.55, 108.15, 114.20, 116.12, 119.89, 126.06, 127.58, 128.28, 129.25, 131.31, 132.08, 137.30, 142.72, 169.33. HRMS (*m/z*): $[M+H]^+$ calcd for $C_{15}H_{12}N_4SCl_2$: 351.0232; found: 351.0236.

4-(2,4-Difluorophenyl)-2-(2-((1-methylpyrrol-2-yl)methylene)hydrazineyl)thiazole (2d): Yield: 76 %, M.P.= 162.4 °C. ^{1}H-NMR (400 MHz, DMSO-d_6): δ: 3.86 (3H, s, CH_3), 6.08 (1H, s, Aromatic CH), 6.42 (1H, s, Aromatic CH), 6.95 (1H, s, Aromatic CH), 7.16-7.20 (2H, m, Aromatic CH), 7.32-7.37 (1H, m, Aromatic CH), 8.01-8.05 (2H, m, Aromatic CH, CH=N). ^{13}C-NMR (100 MHz, DMSO-d_6): δ= 36.92 (CH_3), 104.99, 105.33, 107.66, 108.51, 112.20, 112.36, 114.67, 122.36, 127.41, 128.29, 130.84, 136.25, 144.66, 168.33. HRMS (*m/z*): $[M+H]^+$ calcd for $C_{15}H_{12}N_4F_2S$: 319.0824; found: 319.0825.

4-(2,4-Dimethoxyphenyl)-2-(2-((1-methylpyrrol-2-yl)methylene)hydrazineyl)thiazole (2e): Yield: 69 %, M.P.= 219.5 °C. ^{1}H-NMR (400 MHz, DMSO-d_6): δ: 3.81 (3H, s, CH_3), 3.87 (3H, s, OCH_3), 3.90 (3H, s, OCH_3), 6.10 (1H, s, Aromatic CH), 6.46 (1H, s, Aromatic CH), 6.62 (1H, d, *J*=8.68 Hz, Aromatic CH), 6.67 (1H, s, Aromatic CH), 6.98 (1H, s, Aromatic CH), 7.16 (1H, s, Aromatic CH), 7.84 (1H, d, *J*=8.56 Hz, Aromatic CH), 8.05 (1H, s, CH=N). ^{13}C-NMR (100 MHz, DMSO-d_6): δ= 36.89 (CH_3), 55.77, 56.03, 99.13, 100.39, 105.17, 105.53, 106.90, 108.60, 114.89, 118.83, 121.72, 127.33, 128.45, 130.33, 158.20, 160.57. HRMS (*m/z*): $[M+H]^+$ calcd for $C_{17}H_{18}N_4O_2S$: 343.1223; found: 343.1228.

4-(2,4-Dichlorophenyl)-2-(2-((1-methylpyrrol-2-yl)methylene)hydrazineyl)thiazole (2f): Yield: 70 %, M.P.= 158.9 °C. ^{1}H-NMR (400 MHz, DMSO-d_6): δ: 3.86 (3H, s, CH_3), 6.09 (1H, s, Aromatic CH), 6.46 (1H, s, Aromatic CH), 6.97 (1H, s, Aromatic CH), 7.32 (1H, s, Aromatic CH), 7.51 (1H, d, *J*=8.28 Hz, Aromatic CH), 7.70 (1H, s, Aromatic CH), 7.84-7.86 (1H, m, CH=N), 8.09-8.13 (1H, m, Aromatic CH). ^{13}C-NMR (100 MHz, DMSO-d_6): δ= 36.94 (CH_3), 108.65, 109.10, 114.98, 115.17, 127.22, 127.96, 128.63, 130.14, 132.38, 132.88, 133.36, 137.15, 137.54, 168.01. HRMS (*m/z*): $[M+H]^+$ calcd for $C_{15}H_{12}N_4SCl_2$: 351.0232; found: 351.0238.

4-(3-Nitrophenyl)-2-(2-((1-methylpyrrol-2-yl) methylene)hydrazineyl)thiazole (2g): Yield: 71 %, M.P.= 200.6 °C. ^{1}H-NMR (400 MHz, DMSO-d_6): δ: 3.87 (3H, s, CH_3), 6.08 (1H, s, Aromatic CH), 6.43 (1H, s, Aromatic CH), 6.95 (1H, s, Aromatic CH), 7.60 (1H, s, Aromatic CH), 7.70 (1H, t, *J*=7.84 Hz, Aromatic CH), 7.98 (1H, s, CH=N), 8.12 (1H, d, *J*=8.00 Hz, Aromatic CH), 8.29 (1H, d, *J*=7.44 Hz, Aromatic CH), 8.67 (1H, s, Aromatic CH), 11.95 (1H, s, NH). ^{13}C-NMR (100 MHz, DMSO-d_6): δ= 36.94 (CH_3), 106.22, 108.51, 114.75, 120.36, 122.41, 127.39, 128.32, 130.66, 132.01, 136.20, 136.72, 148.56, 148.74, 169.24. HRMS (*m/z*): $[M+H]^+$ calcd for $C_{15}H_{13}N_5O_2S$: 328.0863; found: 328.0867.

2.2. Assay for inhibition of cholinesterase enzyme

Inhibition of cholinesterase enzyme assay was performed as mentioned in previous studies [10,11].

2.3. Antioxidant Activity

2.3.1. Ferrous ion-chelating effect

Ferrous ion-chelating effect activity was performed as mentioned in previous studies [10,11].

2.3.2. DPPH radical scavenging activity

DPPH radical scavenging activity was performed as mentioned in previous studies [10,11].

3. RESULTS AND DISCUSSION

3.1. Chemistry

New thiazole compounds **2a-g** were created for this investigation, as indicated by Scheme 1. It took two stages to synthesize the chemicals. The first step was a reaction between thiosemicarbazide and 1-methyl-1*H*-pyrrole-2-carbaldehyde to create the thiosemicarbazone chemical. In the second stage, chemicals derived from 2-bromoacetophenone interacted with the thiosemicarbazone product from the first step to produce thiazole derivatives.

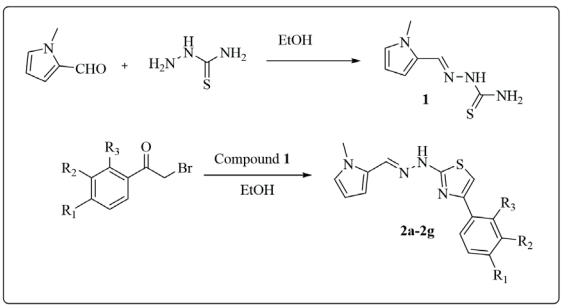

Comp.	R_1	R_2	R_3
2a	-CN	-H	-H
2b	-C_6H_5	-H	-H
2c	-Cl	-Cl	-H
2d	-F	-H	-F
2e	-OCH_3	-H	-OCH_3
2f	-Cl	-H	-Cl
2g	-H	-NO_2	-H

Scheme 1. Chemical structure and general procedure for the synthesis of the final compounds **2a-2g**.

3.2. Cholinesterase Enzymes Inhibition Assay

The results of the *in vitro* inhibition experiments of the obtained thiazole derivative compounds were examined for AChE and BuChE activity. The results obtained for galantamine as the reference drug and all obtained compounds **(2a-2g)** are shown in Table 1. When Table 1 was examined, it was observed that the compounds showed low activity. Among the compounds, the compound **(2e)** with a methoxy group in the *orto* and *para* positions of the phenyl ring showed maximum activity in opposition to AChE by inhibiting 20.32 ± 0.005% at 50 µM concentration. The compound **(2d)** with a fluorine group in the *orto* and *para* positions of the phenyl ring showed maximum level of activity directed toward BuChE by inhibiting 32.54 ± 0.021% at 50 µM concentration.

Table 1. % Cholinesterase inhibitory activities of the synthesized compounds **2a-2g** at 50 µM concentrations

Comp.	AChE	BuChE
2a	NA	7.22 ± 0.019
2b	18.16 ± 0.009	NA*
2c	NA	NA*
2d	11.44 ± 0.007	32.54 ± 0.021
2e	20.32 ± 0.005	NA*
2f	19.06 ± 0.004	NA*
2g	10.74 ± 0.006	23.56 ± 0.016
Gal HBr	97.89 ± 0.01	62.48 ± 0.01

* NA= non-active

3.3. Antioxidant Activity

Antioxidant properties of target compounds were determined by ferric ion chelation and DPPH methods using gallic acid as standard. The obtained values are given in Table 2. When Table 2 is examined, it is seen that the activities of compounds **2e** and **2f** are comparable to the reference drug. Their IC_{50} values are 30.02 ± 0.003 µM and 32.09 ± 0.006 µM, respectively. It is seen that especially compound **2f** shows an activity close to the reference drug gallic acid.

4. CONCLUSION

Seven new thiazole derivatives were synthesized as potential Alzheimer's drugs and their AChE, BuChE inhibition degrees and antioxidant properties were investigated. It was observed that the synthesized compounds did not show sufficient inhibition against AChE and BuChE when compared with the reference drug. The compound with the highest activity against AChE was compound **2e** with a value of 20.32 ± 0.005% at 50 µM concentration. In terms of the antioxidant moiety, compound **2f** showed antioxidant activity similar to the reference drug with an IC_{50} value of 32.09 ± 0.006 µM. According to the obtained results, the molecular docking study was not performed due to the weak activity of the compounds. However, all synthesized compounds can be a reference for new thiazole derivatives to be synthesized for Alzheimer's treatment in the future.

Table 2. DPPH free radical-scavenging activity and ferric ion chelating effect (inhibition % ± S.E.M) of synthesized compounds at 50 µM and IC_{50} values (**µM**)

Comp.	DPPH	ION CHELATING	IC_{50} (DPPH)
2a	NA	NA	> 60 µM
2b	NA	NA	> 60 µM
2c	NA	NA	> 60 µM
2d	11.16 ± 0.007	NA	> 60 µM
2e	68.74 ± 0.003	NA	30.02 ± 0.003
2f	63.18 ± 0.008	NA	**32.09 ± 0.006**
2g	75.64 ± 0.026	NA	24.76 ± 0.008
Gallic Acid	70.29 ± 0.005	-	31.13 ± 0.008
Rutin 50 µM	-	13.21 ± 0.007	-
BHT 50 µM	-	7.06 ± 0.009	-

Ethical approval

Not applicable, because this article does not contain any studies with human or animal subjects.

Author contribution

Conceptualization, Y.Ö.; Supervision, Y.Ö.; Methodology, A.K., T.E. and U.A.Ç.; Data Collection and/or Processing, A.K., T.E. and U.A.Ç.; Analysis and/or Interpretation, U.A.Ç.; Investigation, A.K.; Writing—original draft preparation, Y.Ö., A.K., T.E. and U.A.Ç.; Critical Reviews, Y.Ö. All authors have read and agreed to the published version of the manuscript.

Source of funding

This research received no grant from any funding agency/sector.

Conflict of interest

The authors declared that there is no conflict of interest.

REFERENCES

1. Wiloch MZ, Perez-Estebanez M, Baran N, Heras A, Jönsson-Niedziółka M, Colina A. Spectroelectrochemical studies of TDMQ20: A potential drug against Alzheimer's disease. Bioelectrochem. (2025); 161: 108814. https://doi.org/10.1016/j.bioelechem.2024.108814.
2. Lombardo S, Maskos U. Role of the nicotinic acetylcholine receptor in Alzheimer's disease pathology and treatment. Neuropharmacol. (2015); 96: 255-262. https://doi.org/10.1016/j.neuropharm.2014.11.018.
3. Karran E, Mercken M, Strooper B De. The amyloid cascade hypothesis for Alzheimer's disease: An appraisal for the development of therapeutics. Nat Rev Drug Discov. (2011); 10: 698–712. https://doi.org/10.1038/nrd3505.
4. Liu JM, Yang BY, Zhang XS. Theories of Alzheimer's disease: amyloid hypothesis, blood-brain barrier hypothesis and cholinergic hypothesis. In: E3S Web of Conferences., EDP Sciences. (2024); 553: 05036. https://doi.org/10.1051/e3sconf/202455305036.
5. Sanabria-Castro A, Alvarado-Echeverría I, Monge-Bonilla C. Molecular pathogenesis of Alzheimer's disease: an update. Ann Neurosci. (2017); 24(1): 46–54. https://doi.org/10.1159/000464422.
6. Chen ZR, Huang JB, Yang SL, Hong FF. Role of cholinergic signaling in Alzheimer's disease. Molecules. (2022); 27(6): 1816. https://doi.org/10.3390/molecules27061816.
7. Bekdash RA. The cholinergic system, the adrenergic system and the neuropathology of Alzheimer's disease. Int J Mol Sci. (2021); 22(3): 1273. https://doi.org/10.3390/ijms22031273.
8. Picciotto MR, Higley MJ, Mineur YS. Acetylcholine as a neuromodulator: cholinergic signaling shapes nervous system function and behavior. Neuron. (2012); 76(1): 116–29. https://doi.org/10.1016/j.neuron.2012.08.036.
9. Karakaya A, Çevik UA, Erçetin T, Özkay Y, Kaplancıklı ZA. Synthesis of Imidazole-Thiazole Derivatives as Acetylcholinesterase and Butyrylcholinesterase Inhibitory Activities. Pharm Chem J. (2023); 57(9): 1439–43. https://doi.org/10.1007/s11094-023-03007-8.
10. Ellman GL, Courtney KD, Andres Jr V, Featherstone RM. A new and rapid colorimetric determination of acetylcholinesterase activity. Biochem Pharmacol. (1961); 7(2): 88–95. https://doi.org/10.1016/0006-2952(61)90145-9.
11. Dinis TCP, Madeira VMC, Almeida LM. Action of phenolic derivatives (acetaminophen, salicylate, and 5-aminosalicylate) as inhibitors of membrane lipid peroxidation and as peroxyl radical scavengers. Arch Biochem Biophys. (1994); 315(1): 161–9. https://doi.org/10.1006/abbi.1994.1485.
12. Ercetin T, Senol FS, Orhan IE, Toker G. Comparative assessment of antioxidant and cholinesterase inhibitory properties of the marigold extracts from *Calendula arvensis* L. and *Calendula officinalis* L. Ind Crop Prod. (2012); 36(1): 203–8. https://doi.org/10.1016/j.indcrop.2011.09.007.
13. Blois MS. Antioxidant determinations by the use of a stable free radical. Nature. (1958); 181(4617): 1199–200. https://doi.org/10.1038/1811199a0.

ANADOLU UNIVERSITY
FACULTY OF PHARMACY

European Journal of Life Sciences 2024; 3: 107-113

Research Article

Investigation of the essential oil composition and biological activities of the essential oil and extracts of the aerial parts of *Seseli libanotis* W.D.J. Koch

Burak Temiz[1], Mine Kürkçüoğlu[1], Hale Gamze Ağalar[1,2], Ahmet Duran[3], Kemal Hüsnü Can Başer[4]

[1]Anadolu University, Faculty of Pharmacy, Department of Pharmacognosy, Eskişehir, Türkiye.

[2]Graduate School of Anadolu University, Eskişehir, Türkiye.

[3]Selçuk University, Faculty of Science, Department of Biology, Konya, Türkiye.

[4]Near East University, Faculty of Pharmacy, Department of Pharmacognosy, Lefkosa, North Cyprus.

✉ Burak Temiz
burak_temiz@anadolu.edu.tr

https://doi.org/10.55971/EJLS.1594481

Received: 01.12.2024
Accepted: 24.12.2024
Available online: 31.12.2024

ABSTRACT

In this study, the essential oil and various extracts (*n*-hexane, ethyl acetate, and methanol) were obtained from *Seseli libanotis* W.D.J. Koch aerial parts. The essential oil was obtained via hydrodistillation and subjected to GC and GC/MS analysis. 42 compounds were identified as a major component of acorenone B (43.3%), following by *cis*-sesquisabinene hydrate (9.3%), and *trans*-sesquisabinene hydrate (7.7%). The antioxidant activities of the essential oil and extracts were evaluated using DPPH$^{\bullet}$ and TEAC assays. While the methanol extract exhibited the highest antioxidant activity, no significant tyrosinase inhibition was observed.

Keywords: Antioxidant activity, *Seseli libanotis*, tyrosinase inhibition, volatile constituents

1. INTRODUCTION

The *Seseli* genus belongs to the Apiaceae family and represented in the Flora of Turkey by 10 species. *Seseli libanotis* known as 'moon carrot' or 'mountain stone-parsley' is common in the eastern area of Türkiye. Herb used as a aroma source and preservative in cheese [1,2] and its leaves are consumed as vegetable in eastern Türkiye [3].

Characteristic aroma are associated with its volatile constituents and a few studies have been reported on the composition of essential oils from different parts of plant [1,4-6]. Previous studies has been demonstrated the various biological properties of *S. libanotis* such as antioxidant [7,8], antimicrobial [4-5,8], antiinflamatory [3] activity.

Natural products have long been a significant source of bioactive compounds, serving as an inspiration for drug discovery and development. Among these, essential oils and plant extracts have gained attention due to their distinct chemical compositions and potential pharmacological activities.

In the present study, the essential oil obtained from the aerial parts of *S. libanotis* was analyzed by GC-FID and GC/MS to identify its chemical composition. Additionally, sequential extracts were prepared using hexane, ethyl acetate, and methanol. Antioxidant (DPPH radical scavenging and TEAC) and anti-tyrosinase activities of EO and extracts were evaluated. Furthermore, total phenolic and total flavonoid contents of extracts were determined.

2. MATERIALS AND METHODS

2.1. Plant Material

The aerial parts of *Seseli libanotis* were collected from Artvin, Hatila Valley (forest clearing, 1965 m altitude, 41°07.53'N, 45°35.4'E) on August 18, 2014 (Ahmet Duran, 10027).

2.2. Chemicals and Reagents

All chemicals and solvents were of high purity and at least of analytical grade and purchased from Sigma-Aldrich or Merck.

2.3. Isolation of Essential Oil

The essential oil obtained by hydrodistillation, using a Clevenger-type apparatus for 3h and stored at +4°C in the dark until the analysis.

2.4. Extraction

The extracts were prepared using the maceration method with sequential extraction employing solvents of increasing polarity (*n*-hexane, ethyl acetate, and methanol). Each extraction step was performed in triplicate using an automatic shaker at 150 rpm under room temperature and in darkness for 24 hours. The extracts were concentrated to dryness using a rotary evaporator (<40 °C), and their yields were calculated as 3.6%, 3.5%, and 8.9% for hexane, ethyl acetate, and methanol extracts, respectively.

2.5. GC and GC/MS Analysis

An Agilent 6890N GC system (Agilent, USA; SEM Ltd., Istanbul, Türkiye) was used for GC studies. FID temperature was adjusted to 300°C and the same operating conditions were applied to the same column used in GC/MS analysis. Simultaneous auto injection was employed to obtain equivalent retention times. Relative percentages were determined from integration of the peak areas in the chromatograms.

An Agilent 5975 GC-MSD system was used to perform GC/MS analysis. Chromatographic separation was perfomed by using Innowax FSC column (60m x 0.25mm, 0.25µm film thickness) with helium as carrier gas (0.8 mL/min.). Temperature of oven was adjusted at 60°C for 10 min and programmed to 220°C at a rate of 4°C/min, and kept constant at 220°C for 10 min and then programmed to 240°C at a rate of 1°C/min. The interphase temperature was at 280°C. Split ratio was 40:1 and the injector temperature was set to 250°C. MS were taken at 70 eV between the mass range *m/z* 35 to 450.

2.6. Identification of Compounds

Mass spectra of the components were compared with in-house Baser Library of Essential Oil Constituents, Adams Library [9], MassFinder Library [10], Wiley GC/MS Library [11], and determined by retention indices. These identifications were obtained by comparing their relative retention index (RRI) to a set of *n*-alkanes or retention times with authentic samples [12]. FID chromatograms were used to determine the relative percentage quantities of the separated constituents.

2.7. Antioxidant Activities

The antioxidant activities of the samples were assessed using the DPPH$^{\bullet}$ scavenging and Trolox equivalent antioxidant capacity (TEAC) methods. For DPPH$^{\bullet}$ activity, the method described by Ağalar and Temiz (2021) was employed [13]. Briefly, 8-fold serially diluted samples were incubated with 0.2 mM DPPH$^{\bullet}$ solution for 30 minutes in the dark, and absorbance was recorded at 517 nm. Gallic acid was used as a positive control.

The TEAC assay, following the method of Re et al. (1999), utilized ABTS+$^{\bullet}$ radicals generated by mixing 7 mM ABTS+$^{\bullet}$ and 2.5 mM potassium persulfate, which were left to react for 16 hours in the dark [14]. Samples were mixed with ABTS+$^{\bullet}$, and absorbance was measured at 734 nm after 30 minutes. Results were expressed as Trolox equivalent antioxidant capacity (mmol/L Trolox).

2.8. Total Phenolic and Total Flavonoid Content

Folin-Ciocalteu method was employed to determine the phenolic content [15]. The calibration curve ($y=0.853x + 0.0988$, $R^2 = 0.9994$) was prepared from various concentrations of gallic acid (1-0.8-0.6-0.4-0.2-0.1 mg/mL) and results were expressed as mg gallic acid equivalent (GAE).

$AlCl_3$ method was used to measure the flavonoid content and the absorbances were recorded at 410 nm [16]. Different concentration of quercetin (1-0.8-0.6-0.4-0.2-0.1 mg/mL) ($y = 1.7604x + 0.0251$, $R^2 = 0.9983$) was prepared to create the calibration. Results were calculated as mg quercetin equivalent (QE).

2.9. Tyrosinase Inhibition

The tyrosinase inhibitory activity of the EO and extracts was evaluated by using L-DOPA [17]. Enzyme (200U/mL) and substrate (5 mM) were dissolved in the 0.1 M phosphate buffer (pH 6.8). Briefly, 20 µL sample and 20 µL enzyme was incubated at 25 ˚C for 10 min. Then, reaction was initiated by adding 160 µL L-DOPA and incubated at 25 ˚C for 10 min. Absorbance at 475 nm of each well was measured and kojic acid used as positive control.

2.10. Statistical Analysis

All the experiments were permormed in triplicate, and data were expressed as means ± standard deviation (SD) by using Sigmaplot 14.0 software (Systat Software, Inc., San Jose, CA, USA). IC_{50} values were calculated by regression analysis.

3. RESULTS AND DISCUSSION

3.1. Chemical Composition of *Seseli libanotis* EO

The EO of *Seseli libanotis* was analysed by GC-FID, and GC/MS systems, simultaneously. The essential oil yield was calculated as 0.48% (*v/w*). Fourty-two constituents were determined as representing 92 % of the EO. The most abundant compound was acorenone B (43.3%), making it the major component of the oil. In the literature, aceorenone B has been identified as a major component of the essential oils of plants such as *Niphogeton dissecta* (Benth) J.F. Macbr, *Euphorbia maccorrhiza*, and *Acorus calamus* L., and it has been particularly associated with cholinesterase inhibition properties [18-20]. Other significant constituents included *cis*-sesquisabinene hydrate (9.3%) and *trans*-sesquisabinene hydrate (7.7%), both of which are oxygenated sesquiterpenes and contribute to the chemical complexity of the oil. The oil also contained spathulenol (2.7%) and humulene epoxide-II (2.3%), along with smaller amounts of caryophyllene oxide (1.9%) and carotol (1.2%), indicating a high prevalence of oxygenated sesquiterpenes. Monoterpenes were present in lower concentrations, with α-pinene (0.5%) and limonene (0.2%) being the most prominent compounds (Table 1).

The essential oil composition of *Seseli libanotis* varies considerably depending on the plant part and extraction method used. Skalicka-Wozniak et al. (2010) analyzed the essential oil from fruits using hydrodistillation and HS-SPME, identifying sabinene and *β*-phellandrene as the dominant compounds, particularly in HS-SPME extracts where sabinene reached 46.2% [5]. Furthermore, Masoudi et al. (2006) reported the acorenone (35.5%) as the major volatile substance alongside limonene and α-pinene [6]. Ozturk and Ercisli (2006) found that *trans*-caryophyllene, spathulenol, and caryophyllene oxide was the major components of the aerial parts [4]. The study of Chizzola et al. (2019) revealed that the germacrene D was prevalent in leaves and stems, while fruits were conteined higher amounts of *β*-phellandrene and acorenone B [1]. Additionally, their root volatiles indicated a dominance of *α*-pinene. In the present study, acorenone B was identified as the major component of aerial parts. These differences could associated with chemodiversity of *S. libanotis*, influenced by plant part and geographic origin.

3.2. Antioxidant Activities of Oil and Extracts

The DPPH radical scavenging assay revealed that the methanol extract with a IC_{50} value of 65.2 µg/mL, indicating the highest radical scavenging activity among the tested samples. The ethyl acetate extract showed an IC_{50} value of 480.3 µg/mL. In contrast, the hexane extract and essential oil exhibited limited activity, with IC_{50} values exceeding 2500 µg/mL and 7500 µg/mL, respectively (Table 2).

The TEAC assay provided similar results, with the methanol extract displaying the highest Trolox equivalent antioxidant capacity (1.51 ± 0.02 mM), followed by the ethyl acetate extract (1.00 ± 0.07 mM) and hexane extract (0.34 ± 0.01 mM). The essential oil did not show significant TEAC activity.

Table 1. Chemical composition of the essential oil of *S. libanotis*

RRI	Compounds	%	IM
1032	α-Pinene	0.5	t_R, MS
1118	β-Pinene	0.1	t_R, MS
1132	Sabinene	0.1	t_R, MS
1159	δ-3-Carene	0.2	t_R, MS
1203	Limonene	0.2	t_R, MS
1218	β-Phellandrene	0.1	t_R, MS
1280	*p*-Cymene	1.0	t_R, MS
1528	α-Bourbonene	tr	MS
1568	*trans*-α-Bergamotene	tr	MS
1589	α-Cedrene	tr	MS
1590	Bornyl acetate	tr	t_R, MS
1591	β-Funebrene (=1,7-diepi-β-cedrene)	0.9	t_R, MS
1600	β-Elemene	2.2	MS
1661	Sesquisabinene	0.6	t_R, MS
1668	*(Z)*-β-Farnesene	0.2	MS
1687	α-Humulene	0.3	t_R, MS
1690	α-Acoradiene	0.2	MS
1694	β-Acoradiene	0.2	MS
1703	γ-Curcumene	0.1	MS
1704	γ-Muurolene	0.2	MS
1726	7-epi-1, 2-Dehydro sesquicineole	1.9	MS
1740	Valensene	0.1	t_R, MS
1741	β-Bisabolene	0.4	t_R, MS
1747	Sesquicineole	0.2	MS
1755	β-Curcumene	0.1	MS
1786	*ar*-Curcumene	2.0	MS
1787	Kessane	0.9	MS
2000	*trans*-Sesquisabinene hydrate	7.7	MS
2008	Caryophyllene oxide	1.9	t_R, MS
2045	Carotol	1.2	MS
2071	Humulene epoxide-II	2.3	MS
2096	*cis*-Sesquisabinene hydrate	9.3	MS
2144	Spathulenol	2.7	t_R, MS
2162	α-Acorenol	1.8	MS
2200	*trans*-Methyl isoeugenol	3.1	MS
2228	Acorenone B	43.3	MS
2232	α-Bisabolol	0.4	t_R, MS
2273	Selina-11-en-4α-ol	0.6	MS

RRI: Relative retention indices calculated against n-alkanes; %: calculated from the FID chromatograms; tr:Trace (<0.1 %). Identification method (IM): tR, identification based on the retention times of genuine compounds on the HP Innowax column; MS, identified on the basis of computer matching of the mass spectra with those of the in-house Baser Library of Essential Oil Constituents, Adams, MassFinder and Wiley libraries and comparison with literature data.

Table 1. Continued

RRI	Compounds	%	IM
2404	*trans*-Isoelemicine	1.0	MS
2415	Veratr-aldehyde (=3,4-dimethoxy benzaldehyde) (= Methyl vanillin)	1.6	MS
2471	Veratryl acetone (= 3,4-dimethoxy phenyl acetone)	0.9	MS
2931	Hexadecanoic acid	1.5	MS
	Grouped compounds (%)		
	Monoterpene hydrocarbons	2.2	
	Oxygenated monoterpenes	0	
	Sesquiterpene hydrocarbons	7.5	
	Oxygenated sesquiterpenes	73.3	
	Others	9	
	TOTAL %	**92**	

RRI: Relative retention indices calculated against n-alkanes; %: calculated from the FID chromatograms; tr:Trace (<0.1 %). Identification method (IM): tR, identification based on the retention times of genuine compounds on the HP Innowax column; MS, identified on the basis of computer matching of the mass spectra with those of the in-house Baser Library of Essential Oil Constituents, Adams, MassFinder and Wiley libraries and comparison with literature data.

Table 2. Biological activity properties of *S. libanotis* EO and extracts

	TPC ($mg_{GAE}/g_{extract}$)	TFC ($mg_{QE}/g_{extract}$)	DPPH$^{\cdot}$ (IC_{50}, µg/mL)	TEAC ($mM_{eq.}/g_{ext.}$)	Tyrosinase inhibition %
Hexane ext	22.7 ± 1.4	nd	> 2500	0.34 ± 0.01	nd
EtOAc ext	36.6 ± 0.3	1.1 ± 0.05	480.3 ± 5.1	1 ± 0.07	nd
MeOH ext	72.4 ± 1.03	5.7 ± 0.2	65.2 ± 0.6	1.51 ± 0.02	nd
EO	-	-	> 7500	nd	nd
Gallic acid[c]			1.93 ± 0.02		
Kojic acid[c]					14.28 ± 0.6

Data was given as mean ± SD (*n = 3*). nd: not detected; -: not performed; [c]: Positive controls, values represented IC_{50}, µg/mL).

These results corroborate the DPPH findings, further emphasizing the superior antioxidant capacity of the methanol extract (Table 2).

The antioxidant activities of *S. libanotis* extracts have been extensively evaluated. The methanol extract of the aerial parts demonstrated strong DPPH radical scavenging activity with an IC_{50} of 0.187 mg/mL, while the ethyl acetate extract exhibited moderate activity with an IC_{50} of 0.75 mg/mL [7]. In another study, the methanol extract of *S. libanotis* aerial parts showed notable antioxidant properties with an IC_{50} of 0.46 mg/mL in the DPPH$^{\cdot}$ and ABTS scavenging activity ranging from 1.98 to 2.06 $mg_{VitCequivalent}/g$ [8].

3.3. Total phenolic and flavonoid content

Methanol extract was found to be highest phenolic (72.4 ± 1.03 $mg_{GAE}/g_{extract}$) and flavonoid (5.7 ± 0.2 $mg_{QE}/g_{extract}$) content followed by the ethyl acetate extract with a value of 36.6 $mg_{GAE}/g_{extract}$ and 1.1 ± 0.05 $mg_{QE}/g_{extract}$, respectively. The hexane extract presented the lowest phenolic content (22.7 $mg_{GAE}/g_{extract}$), while flavonoid content was not observed (Table 2). In the study reported by Matejić et al. (2012), methanol extracts of *Seseli libanotis* was studied in terms of phenolic and flavonoid content and results were determined as 85.03 $mg_{GAE}/g_{extract}$, and 12.42 $mg_{QE}/g_{extract}$, respectively [8].

3.4. Tyrosinase inhibiton

Tyrosinase inhibitory properties of extracts and essential oil of *Seseli libanotis* aerial parts were studied for the first time. However, there was no significant activity in tested concentration of samples (Table 2). Therefore, the components of *S. libanotis* may not interact effectively with tyrosinase or lack the necessary chemical features for enzyme inhibition.

4. CONCLUSION

This study provides the comprehensive investigation into the essential oil composition and biological activities of *Seseli libanotis* W.D.J. Koch aerial parts. GC and GC/MS analysis revealed that the acerenone B were the major component of volatile constituents and the sesquiterpenes were exhibited highest content of essential oil. Extracts and the essential oil were evaluated for their antioxidant activities and the methanol extract exhibited the strongest antioxidant properties for both DPPH radical scavenging and TEAC assays. Furthermore, this was the first study on *S. libanotis* EO and extracts for tyrosinase inbition even though no significant effect was observed. Results suggest that the constituents may lack the necessary structural characteristics for tyrosinase interaction. These findings contribute valuable chemical and biological insights into *S. libanotis*, offering a basis for further research into its potential applications in pharmaceutical, cosmetic, and industrial fields.

Ethical approval

Not applicable, because this article does not contain any studies with human or animal subjects.

Author contribution

Conceptualization: B.T., M.K., H.G.A.; Methodology: B.T., H.G.A., M.K.; Supervision: K.H.C.B.; Materials: A.D.; Data Collection and/or Processing: M.K., B.T.; Analysis and/or Interpretation: M.K., B.T.; Literature Search: B.T., M.K., H.G.A.; Writing—original draft preparation: B.T., M.K., H.G.A., K.H.C.B.; Critical Reviews: K.H.C.B. All authors have read and agreed to the published version of the manuscript.

Source of funding

This research received no grant from any funding agency/sector.

Conflict of interest

The authors declared that there is no conflict of interest.

REFERENCES

1. Chizzola R. Chemodiversity of essential oils *in Seseli libanotis* (L.) WDJ Koch (Apiaceae) in Central Europe. Chem Biodivers, (2019);16(6):e1900059. https://doi.org/10.1002/cbdv.201900059
2. Ozturk A, Ozturk S, Kartal S. The characteristics and uses of herbs added to herby cheeses in Van. Herb J Syst Bot, (2000);7:167-181.
3. Küpeli E, Tosun A, Yesilada E. Anti-inflammatory and antinociceptive activities of *Seseli* L. species (Apiaceae) growing in Turkey. J Ethnopharmacol, (2006);104:310-314. https://doi.org/10.1016/j.jep.2005.09.021
4. Ozturk S, Ercisli S. Chemical composition and *in vitro* antibacterial activity of *Seseli libanotis*. World J Microbiol Biotechnol, (2006);22:261-265. https://doi.org/10.1007/s11274-005-9029-9
5. Skalicka-Wozniak K, Los R, Glowniak K, Malm A. Comparison of hydrodistillation and headspace solid-phase microextraction techniques for antibacterial volatile compounds from the fruits of *Seseli libanotis*. Nat Prod Commun, (2010);5(9):1934578X1000500916. https://doi.org/10.1177/1934578X1000500916
6. Masoudi S, Esmaeili A, Khalilzadeh MA, Rustaiyan A, Moazami N, Akhgar MR, Varavipoor M. Volatile constituents of *Dorema aucheri* Boiss., *Seseli libanotis* (L.) WD Koch var. *armeniacum* Bordz., and *Conium maculatum* L.: Three Umbelliferae herbs growing wild in Iran. Flavour Fragr J, (2006);21(5):801-804. https://doi.org/10.1002/ffj.1722
7. Önder A, Cinar AS, Sarialtin SY, Izgi MN, Çoban T. Evaluation of the antioxidant potency of *Seseli* L. species (Apiaceae). Turk J Pharm Sci, (2020);17(2):197. 10.4274/tjps.galenos.2019.80488

8. Matejić J, Džamić A, Mihajilov-Krstev T, Ranđelović V, Krivošej Z, Marin P. Total phenolic content, flavonoid concentration, antioxidant and antimicrobial activity of methanol extracts from three *Seseli* L. taxa. Open Life Sci, (2012);7(6):1116-1122. https://doi.org/10.2478/s11535-012-0094-4

9. Adams RP. Identification of Essential Oil Components by Gas Chromatography/Mass Spectrometry. Allured Publ. Corp, Carol Stream, IL. (2007) ISBN 978-1-932633-11-4

10. Hochmuth DH. MassFinder-4, Hochmuth Scientific Consulting, Hamburg, Germany. (2008).

11. McLafferty FW, Stauffer DB. The Wiley/NBS Registry of Mass Spectral Data, J.Wiley and Sons: New York. (1989).

12. Curvers J, Rijks J, Cramers C, Knauss K, Larson P. Temperature programmed retention indexes: calculation from isothermal data. Part 1: Theory. J High Resolut Chromatogr. 1985;8: 607–610. https://doi.org/10.1002/jhrc.1240080926

13. Agalar HG, Temiz B. HPTLC-DPPH• and HPTLC-tyrosinase methods for hot water-soluble contents of kumquat, limequat and Mexican lime fruit powders. J Res Pharm. (2021); 25(5):569-580. https://doi.org/10.29228/jrp.48

14. Re R, Pellegrini N, Proteggente A, Pannala A, Yang M, Rice-Evans C. Antioxidant activity applying an improved ABTS radical cation decolorization assay. Free Radic Biol Med. (1999);26(9-10):1231-1237. https://doi.org/10.1016/S0891-5849(98)00315-3

15. Singleton VL, Orthofer R, Lamuela-Raventós RM. Analysis of total phenols and other oxidation substrates and antioxidants by means of Folin-Ciocalteu reagent. Methods Enzymol, (1999);299:152-178. https://doi.org/10.1016/S0076-6879(99)99017-1

16. Miliauskas G, Venskutonis PR, van Beek TA. Screening of radical scavenging activity of some medicinal and aromatic plant extracts. Food Chem, (2004);85:231-237. https://doi.org/10.1016/j.foodchem.2003.05.007

17. Likhitwitayawuid K, Sritularak B. A new dimeric stilbene with tyrosinase inhibitory activity from *Artocarpus gomezianus.* J Nat Prod, (2001);64(11):1457-1459. https://doi.org/10.1021/np0101806

18. Calva J, Bec N, Gilardoni G, Larroque C, Cartuche L, Bicchi C, Montesinos JV. Acorenone B: AChE and BChE inhibitor as a major compound of the essential oil distilled from the Ecuadorian species *Niphogeton dissecta* (Benth.) JF Macbr. Pharmaceutics, (2017);10(4):84. https://doi.org/10.3390/ph10040084

19. Lin J, Dou J, Xu J, Aisa HA. Chemical composition, antimicrobial and antitumor activities of the essential oils and crude extracts of *Euphorbia macrorrhiza*. Molecules, (2012);17(5):5030-5039. https://doi.org/10.3390/molecules17055030

20. Süzgeç-Selçuk S, Özek G, Meriçli AH, Baser KHC, Haliloglu Y, Özek T. Chemical and biological diversity of the leaf and rhizome volatiles of *Acorus calamus* L. from Turkey. J Essent Oil Bear Plants, (2017);20(3):646-661. https://doi.org/10.1080/0972060X.2017.1331142

ANADOLU UNIVERSITY
FACULTY OF PHARMACY

European Journal of Life Sciences 2024; 3: 114-126

Review Article

An examination of natural and synthetic tyrosinase inhibitors

Gizem Demirdiş[1]

[1]Eskişehir Technical University, Department of Chemistry, Eskişehir, Türkiye.

✉ Gizem Demirdiş
gizemtutar@eskisehir.edu.tr

https://doi.org/10.55971/EJLS.1498811

Received: 10.06.2024
Accepted: 21.11.2024
Available online: 31.12.2024

ABSTRACT

The enzyme responsible for this process is known as tyrosinase, which is sometimes referred to as polyphenol oxidase, monophenol oxidase, phenolase, or catecholase. It is present in humans, plants, microbes, and fungi. Melanin pigments, found in both plants and animals, require this enzyme as an essential component. Tyrosinase is present in animal creatures, particularly in the pigments of the skin, hair, and eyes. Tyrosinase can cause darkening in foods that is unrelated to their inherent color. Beverages such as fruit juice and wine may experience a decline in appearance and flavor, as well as the occurrence of turbidity and precipitation. The unwanted phenomenon of browning in fruits and vegetables, which is frequently caused by enzymatic processes, needs to be avoided. Tyrosinase enzyme inhibitors are employed to hinder the catalytic oxidations that lead to browning by the tyrosinase enzyme. Currently, these basic ingredients are commonly found in skin whitening solutions, particularly in the field of cosmetics. In addition, tyrosinase inhibitors have practical applications in the treatment of skin problems associated with melanin pigmentation. Furthermore, tyrosinase inhibitors competitively and reversibly hinder the activity of human melanocyte tyrosinase, hence impeding the production of melanin.

Numerous substances possess the ability to hinder the activity of the enzyme tyrosinase. Ongoing studies are being conducted on several derivatized compounds to increase inhibition. This article explores the inhibitory effects of many compounds, including kojic acid, azelaic acid, flavonoids, arbutin-deoxyarbutin, curcumin and its derivatives, and copper chelators, on the enzyme tyrosinase.

Keywords: Azelaic acid, flavonoids, inhibitors, kojic acid, tyrosinase

1. INTRODUCTION

Tyrosinase (EC 1.14.18.1) is an important member of the polyphenoloxidase enzymes, containing the amino acid histidine in its active site. Tyrosinase is a metalloenzyme that possesses two copper atoms as cofactors. Tyrosinase is an enzyme that catalyzes the oxidation of monophenols (monophenolase activity) and *o*-diphenols (diphenolase activity) to reactive oquinones. Both tyrosinase activities exhibit wide substrate specificities, however they display a greater preference for L-isomers as substrates compared to D-isomers. Since the initial biochemical studies, it has been discovered that the enzyme is widely distributed, ranging from bacteria to mammals. The most extensively studied tyrosinases are obtained from *Streptomyces glausescens*, *Neurospora crassa*, and *Agaricus bisporus*. The central copper-binding domain of tyrosinase, which has conserved amino acid residues, including three histidines, is the most significant characteristic seen in the enzyme from many sources. A tyrosinase molecule can

accommodate a pair of copper atoms, with each atom of the bidentate copper cluster forming chemical bonds with three histidines [1].

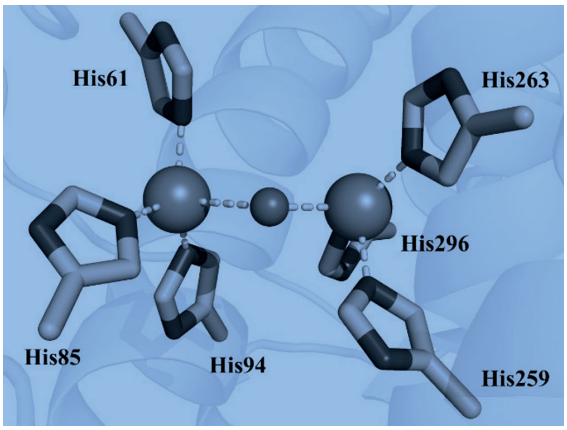

Figure 1. Active site of the crystal structure of *Agaricus bisporus* mushroom tyrosinase (Protein Data Bank, PDB ID 2Y9W) [2].

Tyrosinase is an enzyme that is present in many different kinds of organisms and is essential for the creation of melanin pigments. The enzyme tyrosinase helps plants make lignin, which is important for their defense mechanisms and growth. Factors in the environment, heavy metal exposure, and ultraviolet (UV) radiation can all increase tyrosinase activity. Plants protect themselves from oxidative stress through the antioxidant chemicals phenolic and flavonoid, which are produced in response to tyrosinase activity. Furthermore, it causes plants to undergo enzymatic browning [3]. Apart from inducing enzymatic browning in plants, it also causes animals to produce melanin. Mammals have melanin in their hair, eyes, skin, and inner ears. It plays a vital role in pigmentation. The biological process known as melanogenesis is responsible for the synthesis of melanin, an intricate polymer possessing an indolic structure. The pigment melanin is the cause of the different skin tones that people have. It is also essential for protecting skin from the sun's harmful UV radiation. Melanocytes contain specialized organelles called melanosomes, which are where the process of creating melanin takes place. The critical catalytic step that regulates the rate at which melanin is produced is controlled by the enzyme tyrosinase. Tyrosinase-induced hyperpigmentation can lead to a number of skin disorders, such as melasma, age spots, freckles, and malignant melanoma.

This enzyme is essential for the proper functioning of melanin pigments, which can be found in numerous plant and animal species. Melanin biosynthesis is catalyzed by it in three steps: (i) tyrosine undergoes hydroxylation to form 3,4-dihydroxyphenylalanine (DOPA); (ii) DOPA is oxidized to dopakinone; and (iii) indolequinone is produced by oxidation of 5,6-dihydroxyindole (DHI). The reaction changes two types of melanin into completely different substances. A brownish-black pigment called eumelanin and a reddish-yellow pigment called pheomelanin are both present; eumelanin is insoluble in water and possesses a polymer structure [4]. Figure 2 shows the process, which includes various complex enzymatic reactions.

Melanin synthesis regulation involves three critical enzymes. Three proteins: human tyrosinase (hTYR), tyrosinase-related protein-1 (TYRP-1), and tyrosinase-related protein-2 (TYRP-2). A copper center distinguishes hTYR from TYRP-1 and TYRP-2, which both contain two zinc centers. Nitric oxide, MAPK, MC1R/a, PI3K/Akt, Wnt/b-catenin, and other signaling pathways within melanocytes regulate melanogenesis. Overactive or activated tyrosinase could be the consequence of signaling pathway disruption. Albinism and vertigo are disorders caused by a decrease in the functionality of the enzyme tyrosinase and related enzymes.

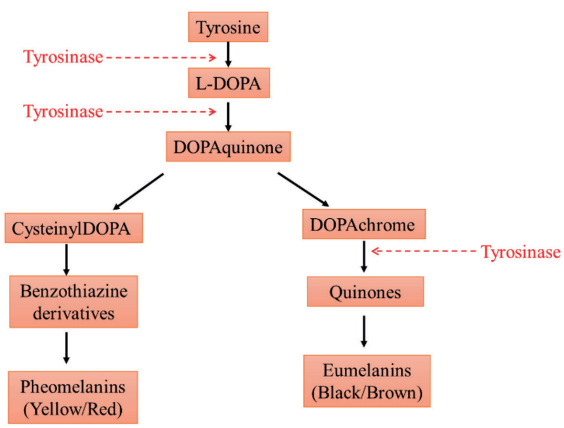

Figure 2. Tyrosinase enzyme pathway of melanin synthesis

When this gene is overexpressed, it can cause hyperpigmentation, which manifests as brown spots, age spots, freckles, and the like. A person's standard of living may suffer as a result of this. Furthermore, it has the ability to develop into malignant melanoma, an extremely dangerous and difficult-to-treat skin cancer that can be fatal if left untreated [5].

The study of enzymes and their applications is an evolving discipline. There has been a lot of study into the best ways to isolate and purify enzymes from plants and animals, particularly in the last several years. The tyrosinase enzyme has numerous uses in food, health, cosmetics, agricultural, and other related industries due to its involvement in numerous critical reactions. Being present in so many different types of produce gives it a significant foothold in the food business [6].

It catalyzes reactions of oxidation of phenolic compounds leading to the formation of pigments responsible for color changes in fruits, vegetables or processed food products. In the food industry, it causes adverse appearance and taste changes, turbidity and precipitation in beverages such as fruit juice, causing damage. Tyrosinase inhibitors are used in the food industry to eliminate the undesirable conditions caused by the tyrosinase enzyme. In addition, the activity of the tyrosinase enzyme is important to enhance the color and flavor of foodstuffs such as dried fruits, coffee, tea, cocoa [7].

Abnormal production of melanin pigment causes significant aesthetic issues because it is involved in melanin formation. Because of their capacity to prevent the enzymatic browning of food items and their skin-lightening effects, tyrosinase inhibitors find widespread use in the cosmetics industry. Additionally, neurodegeneration has been associated with Parkinson's disease, and tyrosinase has been found to induce dopamine neurotoxicity. A degeneration of dopaminergic neurons in the brain causes Parkinson's disease, a neurodegenerative condition. So, many Parkinson's disease drugs and studies have focused on blocking tyrosinase [8].

Because tyrosinase is a copper chelators such as aromatic acids, non-aromatic chemicals phenolic ingredients, can compete to inhibit the enzyme [4]. Numerous tyrosinase inhibitors have been found naturally and synthetically. Hydroquinone, α-arbutin, kojic acid, retinoids, azelaic acid, resveratrol, camptaric acid, chrysosplenetin and phenylethyl resorcinol have been identified as tyrosinase inhibitors [9].

2. TYROSINASE INHIBITORS

In many studies in the literature, inhibitors are evaluated in the presence of tyrosine or DOPA, the substrate of the enzyme, in terms of DOPA-chrome formation. Tyrosinase inhibitors are mainly used

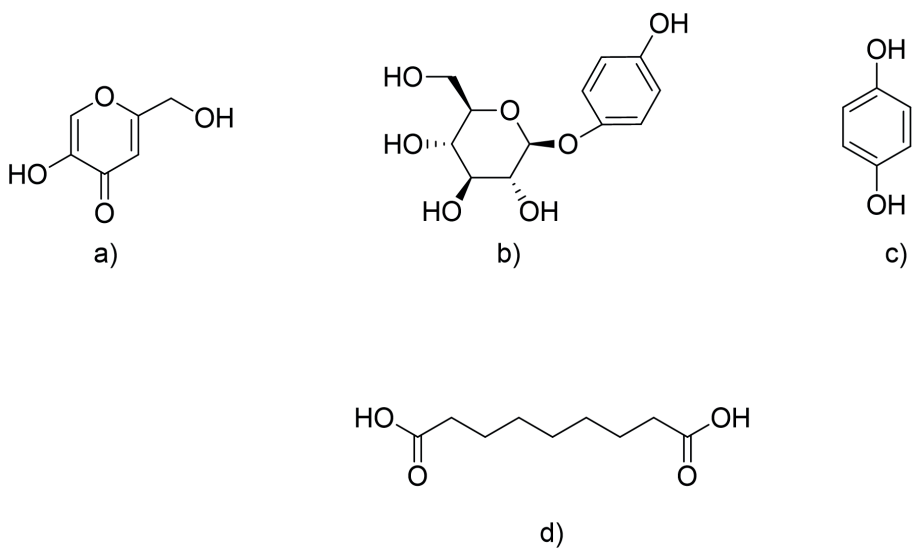

Figure 3. Tyrosinase inhibitors chemical structure a) kojic acid, b) arbutin, c) hydroquinone, d) azelaic acid.

in reference to melanogenesis inhibitors, which interfere to some extent with melanin formation.

2.1. Kojic acid and derivatives

Kojic acid (5-hydroxy-2-(hydroxymethyl)-4*H*-pyran-4-one) (Figure 4) is one of the metabolites produced by various strains of fungi or bacteria such as *Aspergillus* and *Penicillium*. Kojic acid, which is often studied as an inhibitor of tyrosinase, is used as a skin whitener in the cosmetics industry and is also used in the food industry to prevent enzymatic browning [1]. Kojic acid shows a competitive inhibitory effect on monophenolase activity and a quasi-competitive inhibitory effect on the diphenolase activity of fungal tyrosinase. The ability of kojic acid to chelate copper in the active site of the enzyme explains its competitive inhibitory effect. The biological activities of kojic acid are attributed to its γ-pyranone structure containing an enolic hydroxyl group. If the enolic hydroxyl group is retained, the tyrosinase inhibitory activity is completely lost. It acts by chelating copper in the active site of the tyrosinase enzyme. Kojic acid is also an antioxidant and scavenges reactive oxygen species that are excessively released from cells or formed in tissue or blood. Stable metal kojic acid complexes are created when kojic acid reacts with metal salts of aluminum, chromium, cobalt, copper, gold, indium, iron, nickel, manganese, palladium, vanadium, and zinc [10-12].

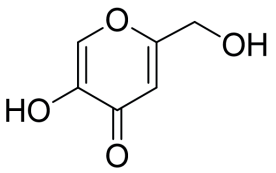

Figure 4. Kojic acid chemical structure

Based on the fact that kojic acid is an inhibitor of tyrosinase enzyme, many derivatives of kojic acid were investigated and its inhibition effect was examined. The low stability of kojic acid has pioneered the search for different derivatives. It has been observed that the C-terminal amine groups in the structure to be involved in the inhibition of tyrosinase enzyme create a high inhibition effect [13,14].

Aromatic side chains can interact with the hydrophobic pocket containing the amino acids His63, His216 and Phe59 surrounding the double-core copper in the active site of the tyrosinase enzyme. As a result, aromatic molecules can exert competitive, semi-competitive and non-competitive inhibition. As a result of conjugation of kojic acid and various amino acids, it was observed that kojic acid-phenyl alanine had a higher inhibition effect than kojic acid and remained stable for more than 3 months [15]. In another study, compounds formed as a result of molecular hybridization of kojic acid and aromatic aldehydes exhibited a strong tyrosinase inhibitory activity. As a result, it was determined that it prevents browning [16].

The hydroxypyranone moiety of kojic acid serves as a scaffold for tyrosinase inhibitors, as it shows the ability to chelate with copper ions in the tyrosinase active center. The enhancement of kojic acid with functional groups showed an inhibition effect 9-fold higher than that of kojic acid [17].

Numerous studies have examined the inhibitory effects of compounds extracted from plant sources, fungi, and microbes on tyrosinase. Despite kojic acid being the most extensively researched compound, its volatility, potential adverse effects from prolonged exposure, and limited efficacy have prompted

researchers to explore derivatives to mitigate these drawbacks.

Shao et al. synthesized hydroxypyridinone derivatives and formulated variants capable of mitigating the adverse effects of kojic acid. The compounds demonstrated superior efficacy in bleaching compared to kojic acid [18].

A cohort of researchers examining the impact of the benzapyrone ring on tyrosinase inhibition synthesized several derivatives by the conjugation of kojic acid and coumarin including the benzapyrone ring. The findings indicated that the compounds conjugated with coumarin had a greater inhibitory impact on tyrosinase than kojic acid [19,20].

2.2. Azelaic acid and derivatives

Azelaic acid is structurally a 9-carbon straight chain 1,7-heptandicarboxylic acid. It is commonly used

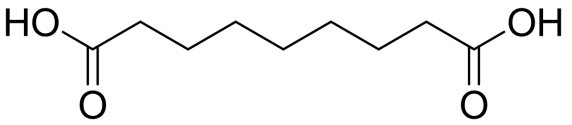

Figure 5. Azelaic acid chemical structure

in the treatment of acne, melanoma, rosacea and hyperpigmentation [21]. Azelaic acid is metabolized by β-oxidation resulting in the formation of malonyl-CoA or acetyl-CoA. Due to its chemical structure, it has the capacity to inhibit tyrosinase and to a much greater extent thioredoxin. Azelaic acid has anti-inflammatory, antibacterial and anti-keratinizing effects and has a significant therapeutic efficacy on acne [22,23].

Azelaic acid inhibits the enzyme tyrosinase. This enzyme is involved in the conversion of tyrosine into DOPA and DOPA-quinone, precursors of melanin. Dicarboxylic acids do not affect normal skin melanocytes, so AZA can be used to treat many types of skin hyperpigmentation and does not cause discoloration of healthy skin near the lesions [23].

In a study with azelaic acid esters, it was found to inhibit the tyrosinase enzyme. It was determined that it completely inhibits L-tyrosine oxidation and stops esterification reactions [24].

2.3. Flavonoids

Flavonoids constitute the principal polyphenolic group in plants, often present in the fruits, vegetables, drinks, and cereals that we eat every day. Flavonoids belong to a class of naturally occurring plant polyphenolic secondary metabolites found in many plants and therefore widely consumed in the diet. In general, they are composed of 15 carbons; a phenyl ring and a heterocyclic ring. Biological studies carried out on natural and synthetic analogues of flavonoids have revealed anti-keratinization, anti-microbial, anti-cancer, anti-inflammatory, anti-ulcer action by these species [25].

Flavonoids, due to their polyhydroxyphenolic structure, are metal chelators that can interact with copper ions in the active site of tyrosinase. Therefore, their species and their derivatives are model compounds for tyrosinase inhibition. Numerous compounds derived from natural products have been reported to be moderate to potent tyrosinase inhibitors [26]. Among these, many flavonoid derivatives have been found to be potent inhibitors of tyrosinase. Four important flavonoid compounds, chrysin, quercetin, naringin and kaempferol, have been shown to play an important role in tyrosinase inhibition [27, 28].

The general structure of flavonoids indicates that keto groups possess significant potential as tyrosinase inhibitors. The -OH group at the C-3 position in the structure is crucial for activity. Flavonoids, including kaempferol and quercetin, possess a 3-hydroxy-4-keto moiety in their structure. This allows it to function as a copper chelator in the inhibition of tyrosinase, thereby obstructing the enzyme's activity. In heterocyclic rings containing 5 or 6 carbon atoms, the presence of -OH and -CH_3 groups, frequently observed around the ring, is indicative of the structure. These groups exhibit an inhibitory effect by influencing the enzymatic activity within the structure [29].

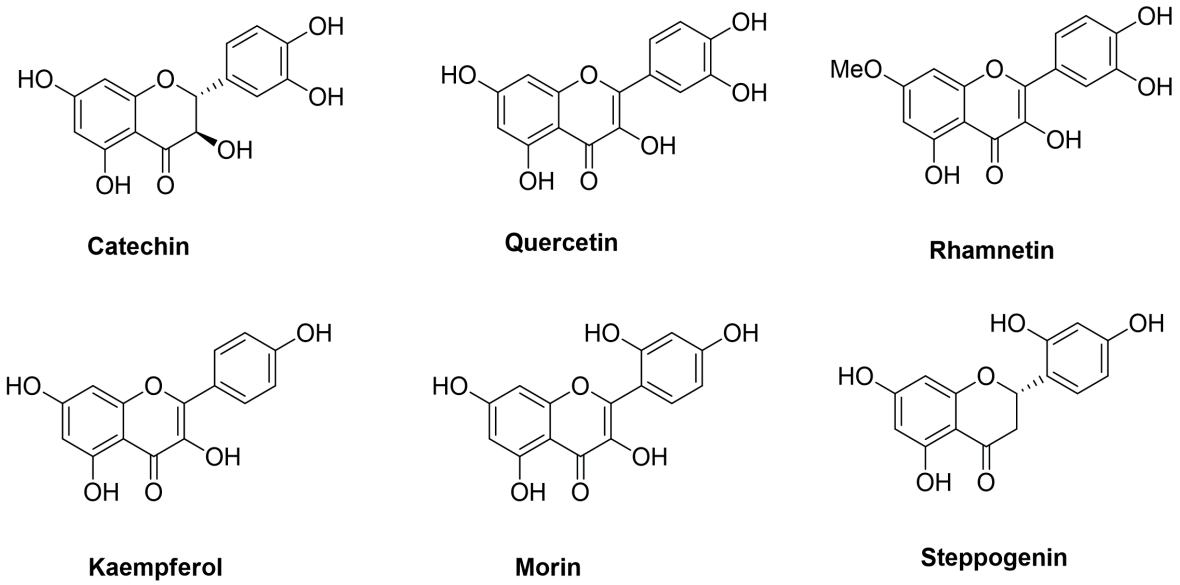

Figure 6. Chemical structures of flavonoids

Chrysin (5,7-dihydroxyflavone) is a natural flavonoid derived from many plants and has anti-melanogenesis effects [30]. Naringin (5,7,4-trihydroxyflavone) is another type of flavonoid with tyrosinase inhibition activity [31]. Quercetin (5,7,3,4-tetrahydroxyflavonol) also shows tyrosinase inhibitory effects through inhibition of diphenolase activity [32]. Rocchitta et al. demonstrated in their study that the structure of quercetin exhibited an inhibitory effect through hydrogen bonding interactions with the His85, His244, Thr261, and Gly281 residues of tyrosinase [20]. Kaempferol (5,7,4-trihydroxyflavonol) is another flavonoid inhibitor whose anti-tyrosinase effects have often been proven [33].

In a study, the tyrosinase inhibition effects of flavonoids such as kaemferol and quercetin were investigated. The compounds competitively inhibited the tyrosinase enzyme and showed a higher inhibition effect than kojic acid [34].

2.4. Arbutin-deoxyarbutin and derivatives

Arbutin (hydroquinone-O-*β*-D-glucopyranoside), a natural polyphenol isolated from the bearberry plant *Arctostaphylos uva-ursi* (L.) Sprengel, has whitening and anticancer properties. Arbutin is a compound in which the D-glucose molecule is linked to hydroquinone. D-glucose exists in aqueous solution in *α*, *β* or *γ*-anomeric form; the compound in which the *β*-anomer of D-glucose binds to hydroquinone is called *β*-Arbutin (this stereoisomer is called arbutin) and the compound in which the α-anomer of D-glucose binds to hydroquinone is called *α*-Arbutin. Both forms of arbutin are hydroxylated at the *ortho* position of the catechol group by oxytyrosinase, resulting in a complex formed by hydroxylated mettyrosinase [35,36].

Due to its glucose composition, arbutin is regarded as more dependable than hydroquinone. Arbutin is highly hydrophilic, so skin penetration is relatively low. Arbutin is resistant to light and unstable at pH 2. Arbutin can undergo partial hydrolysis to hydroquinone in the presence of water, which in turn can be oxidized to benzoquinone [37]. *α*-Arbutin is 10 times more effective than *β*-arbutin in inhibiting tyrosinase, but α-arbutin is easily degraded by heat [37,38].

Deoxyarbutin, another derivative of hydroquinone, is clinically more effective and safer than arbutin in the treatment of hyperpigmentation. Deoxyarbutin is a second generation hydroquinone derivative. Deoxyarbutin is less cytotoxic than other hydroquinone derivatives [39,40].

After removal of all hydroxyls in the glycoside side chain, *β*-arbutin is converted to deoxyarbutin. This

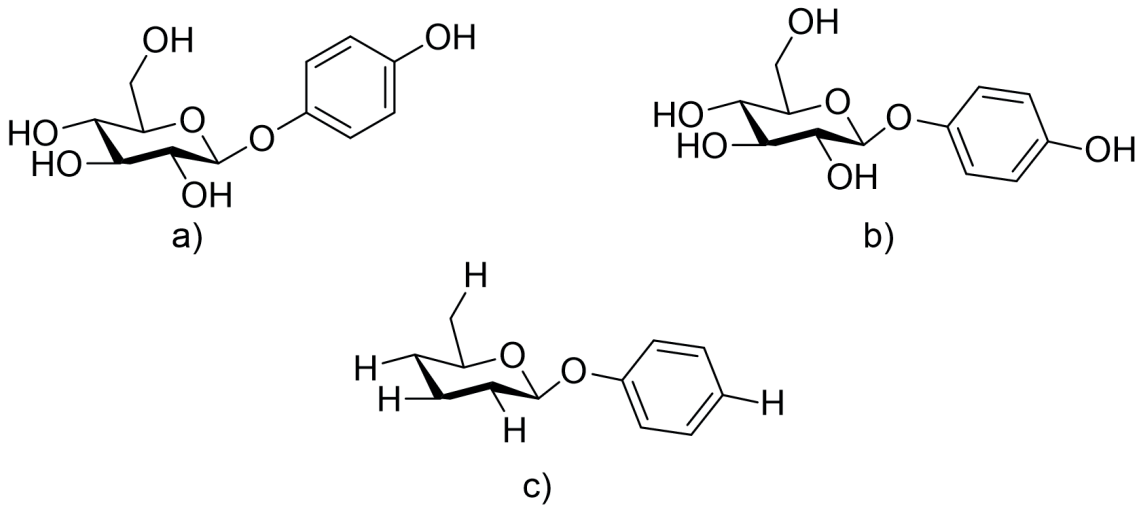

Figure 7. The molecular structure of a) *β*-arbutin, b) *α*-arbutin, c) deoxy-arbutin

procedure results in increased lipo-solubility of deoxyarbutin compared to *β*-arbutin. Deoxyarbutin shows a stronger tyrosinase enzyme inhibition than hydroquinone and *β*-arbutin [41]. The activity of arbutin and its derivatives is related to particle size, spatial structure and electrostatic potential around the benzene ring [42].

Studies have shown that arbutin, deoxyarbutin and their derivatives inhibit the activity of the tyrosinase enzyme and prevent the oxidative polymerization of melanogenic intermediates, which is common for antioxidant compounds that provide protection from reactive oxygen species produced by UV radiation. In addition, arbutin and its derivatives were found to inhibit the maturation of melanoma cells. The *in vitro* study showed that arbutin is gradually oxidized in the presence of tyrosinase, which makes its effect prolonged in the presence of antioxidants such as L-ascorbic acid [42]. In several studies, *α*- and *β*-arbutin inhibited melanin formation in B16 cells induced by α-melanocyte stimulating hormone (α-MSH) and blocked thyronazinase activity [43–45]. Acetylated arbutin exhibits enhanced tyrosinase inhibitory potential, likely due to the increased solubility and improved membrane penetration conferred by the acetyl group in lipid-containing systems [44]. There is reason to be optimistic about the potential of phenolic compound derivatives as tyrosinase inhibitors in the stages of melanomagenesis. By inhibiting the production of melanin in B16F10 cells, the active phenolic and alkylhydroquinone components found in the extract of the *Rhus succedanea* L. tree demonstrated a tyrosinase inhibitor effect. Upon conducting comparisons with hydroquinone, it was determined that the active alkylhydroquinone component exhibited an IC_{50} value of 37 μM. Conversely, the IC_{50} value of hydroquinone was found to be exactly 70 μM. It was observed, as a consequence of the data that was obtained, that the heptadecenyl chain that was present in the structure of the active component was responsible for the oxidation of the hydroquinone ring. As a consequence of this, a more efficient derivative inhibitor molecule was purified from hydroquinone [46].

2.5. Curcumin and derivatives

Curcumin is commonly regarded as a prototypical example of phenylpropanoid compounds due to its chemical structure. The compound is called 1,7-bis(4-Hydroxy-3-methoxyphenyl)-1,6-heptadiene-3,5-dione [47]. Curcumin is a plant-derived polyphenol obtained from *Curcuma longa* L., also known as turmeric. Turmeric is a powdered rhizome of this plant that is commonly used to enhance the color and taste of food. It is also traditionally believed to have medicinal properties for treating inflammatory illnesses and other diseases. Curcumin, also known as diferuloylmethane, possesses both anticancer and tyrosinase enzyme inhibitory effects Curcumin, at

concentrations between 25-110 μM, was discovered to possess inhibitory effects on melanin formation via activating the Akt/PKB signaling pathway. This activation can hinder the process of melanogenesis by decreasing MITF levels and blocking the action of the enzyme tyrosinase [48,49].

Phenolic chemicals, known for their antioxidant properties, can aid in the prevention and relief of various chronic diseases resulting from oxidative stress. Research has demonstrated that curcumin and its derivatives have a greater inhibitory effect on the tyrosinase enzyme compared to kojic acid. Furthermore, research has demonstrated that the *β*-phenyl-*α*, *β*-unsaturated carbonyl structure seen in curcumin derivatives is strongly associated with the ability to block tyrosinase. Coumaric acids are compounds that are derived from mono-hydroxylated cinnamic acid in the phenyl group. Among these compounds, *p*-coumaric acid is the most prevalent type. *p*-Coumaric acid is present in substantial amounts in numerous fruits, vegetables, and cereals. *p*-Coumaric acid is a potent antioxidant known for its ability to eliminate reactive oxygen species (ROS) and free radicals [50,51]. Research has demonstrated that derivatives of *p*-coumaric acid exhibit a distinct ability to inhibit the enzyme tyrosinase [52,53]. Furthermore, *p*-coumaric acids were examined for their impact on melanin creation in B16F10 cells and were observed to decrease melanin production [54].

The polyphenolic content of curcumin has become significant in scientific research focused on its antioxidant properties and potential as an anticancer agent. The literature has examined the effect of curcumin on tyrosinase inhibition, specifically regarding its whitening properties and its implications for melanoma and other skin cancer types [55].

2.6. Copper chelators

The majority of drugs that chelate copper ions in the active site of the tyrosinase enzyme have the ability to inhibit the tyrosinase enzyme. Tropolone is an established tyrosinase inhibitor due to its ability to chelate copper. Tropolone derivatives were synthesized based on the structure of the tiny seven-membered ring, and it was discovered that these derivatives have the ability to block the tyrosinase enzyme [56]. The researchers conducted an investigation on the red tembul leaves to determine the effect of their alkaloids, tannins, and flavonoid content as tyrosinase inhibitors. The results of the investigation show promising outcomes [57].

The study utilized ilapia skin collagen hydrolysate to examine the potential for TYR inhibition. The results indicated that TYR inhibitory peptides had a greater ability to chelate copper [58].

2.7. Resveratrol and derivatives

Resveratrol (3,4',5-trihydroxy-*trans*-stilbene) has been the subject of extensive research over the past decade due to its diverse bioactivities, which include anti-inflammatory and antioxidant properties, as well as effects on cancer, neurodegenerative diseases, and aging. Resveratrol has demonstrated the ability to mitigate neuroinflammation and oxidative stress, primarily through the enhancement of neurotransmitter release. Recent studies indicate that resveratrol exhibits an inhibitory effect on the tyrosinase enzyme [59].

The antioxidant efficacy of resveratrol is contingent upon the redox potential of the phenolic hydroxyl group and the capacity for electron delocalization attributed to its conjugated configuration. The antioxidant mechanism of resveratrol encompasses the reduction of reactive oxygen species (ROS) generation, the scavenging of free radicals, and the enhancement of antioxidant biosynthesis. Moreover, its phenyl ring has lately garnered significant interest owing to its potential chemopreventive and chemotherapeutic properties [60,61].

The bioavailability of resveratrol is limited owing to its chemical instability and poor solubility. The inhibition of tyrosinase by resveratrol derivatives was examined to mitigate these drawbacks [62].

Oxyresveratrol (*trans*-3,5,2′,4′-tetrahydroxystilbene) possesses an additional hydroxyl group, distinguishing it from resveratrol. A study conducted in 2021 demonstrated that oxyresveratrol exhibits a more potent inhibitory effect on tyrosinase activity, attributed to its capacity to form a greater number of hydrogen bonds in comparison to resveratrol [62,63].

2.8. Heterocyclic Compounds and Derivatives Containing Triazole and Thiazole

Heterocyclic compounds are cyclic structures that incorporate oxygen, nitrogen, or sulfur, with at least one heteroatom present. Quintuple-ring aromatic heterocyclic compounds exhibit remarkable stability. Heterocyclic compounds are utilized across various domains. Heterocyclic compounds that contain nitrogen and sulfur are commonly utilized for pharmacological and biological activity. Thiazoles, comprising both nitrogen and sulfur atoms in their rings, are incorporated into numerous pharmaceutical active ingredients as biologically active compounds. Triazoles are five-membered heterocyclic compounds containing three nitrogen atoms. These molecules are often examined for their derivatives because of their biological activity [64–68].

A 2019 study compared the effects of tyrosinase inhibition using kojic acid as a positive control and synthesized a novel heterocyclic amide compound featuring a new triazole and thiazole ring. The researchers investigated the inhibitory effect of the synthesized compound on the fungal tyrosinase enzyme. The presence of two methylene groups in the derivative structure enhanced its activity due to the steric effect. A comparison of the derivative molecule with kojic acid revealed an activity enhancement of approximately 15-20 times. The findings with various derivatives indicated that the polar and bulky substituents on the phenyl ring in the derivative molecules adversely affected the activity. The same research group examined the inhibitory effects of derivatives resulting from modifications at the C-3 and N-4 positions of the triazole ring. They synthesized various derivatives by substituting the ethyl group in the triazole ring with a benzyl group in place of the attached acetamide group. The synthesized heterocyclic derivative compounds exhibited lower IC_{50} values than standard molecules and demonstrated potential as inhibitory agents [65,69,70].

In a further promising study, the synthesized derivative molecule was formed via a hydrogen bond between cysteine and the amino group of the thiazole ring. The interactions between the thiazole ring and histidine were established through hydrogen bond formation. The tyrosinase inhibition studies of this new derivative molecule indicated a promising IC_{50} value in comparison to the standard molecule [71].

Shakila et al. synthesized indole-triazole derivatives incorporating N-acetamide by linking an indole ring to the carbon of the triazole ring. The synthesized compounds were evaluated for their potential as tyrosinase inhibitors, yielding IC_{50} values ranging from 0.033 to 0.142 μM. The IC_{50} values obtained indicated a substantial inhibitory effect, showing a marked difference in comparison to standard molecules [72].

3. CONCLUSION

This study summarizes and critically analyzes studies on isolated compounds with possible tyrosinase inhibitory action. The enzymatic oxidation of phenols by the enzyme tyrosinase is responsible for the browning of nutrients. Consequently, there is a degradation of crucial amino acids, a decrease in the ability to be digested, and a decline in nutritional value, along with the creation of harmful substances. The occurrence of these unwanted browning events is a significant challenge, and it is imperative to explore potent tyrosinase inhibitors to address this issue. Melanin has a crucial function in safeguarding the skin from the development of skin cancer caused by exposure to sunlight. Nevertheless, the excessive synthesis of melanin pigment poses both cosmetic and medicinal concerns in humans. Nevertheless, tyrosinase inhibitors are employed in medical practice to treat some conditions associated with excessive melanin pigmentation, and they also play a significant role in the fields of cosmetics and pharmaceuticals due to their ability to lighten the skin. Numerous natural and synthetic compounds and their derivatives have been shown to inhibit tyrosinase effectively; nevertheless, the majority have not undergone clinical investigation. At now, only a limited number of chemicals are used in topical dermatological formulations. However, there are only a limited number of commercially accessible tyrosinase inhibitors. The limited applicability of

these substances is a result of their high intercellular toxicity and low stability, which raises concerns. This article reviews the capacity of several chemicals to hinder the tyrosinase enzyme, as well as the molecules that can beyond the constraints and exhibit a stronger inhibitory impact. The advancement of inhibitors in the literature and modifications to enhance inhibitor activity are significant considerations. The design of natural or synthetic tyrosinase inhibitors is a significant research topic, driven by considerations of high bioavailability, low cytotoxicity, and effective inhibition. This review examines the inhibitory effects of various derivatives, particularly phenolic and heterocyclic compounds, on tyrosinase activity. It highlights the significance of understanding structural modifications in the identification of new inhibitors. This review aims to provide guidance and a comprehensive strategy for the development of novel, effective, highly active, and safe tyrosinase inhibitors for enhanced practical applications in the future.

Ethical approval

Not applicable because this article does not contain any studies with human or animal subjects.

Author contribution

Conceptualization, G.D.; Data collection and/or processing, G.D.; Investigation, G.D.; Writing—original draft preparation, G.D.; Writing—review and editing, G.D. The author has read and agreed to the published version of the manuscript.

Source of funding

This research received no grant from any funding agency/sector.

Conflict of interest

The author declared that there is no conflict of interest.

REFERENCES

1. Chang T-S. An Updated Review of Tyrosinase Inhibitors. Int J Mol Sci (2009);10:2440–75. https://doi.org/10.3390/ijms10062440.
2. Zou C, Huang W, Zhao G, Wan X, Hu X, Jin Y, et al. Determination of the Bridging Ligand in the Active Site of Tyrosinase. Molecules (2017);22:1836. https://doi.org/10.3390/molecules22111836.
3. Loizzo MR, Tundis R, Menichini F. Natural and Synthetic Tyrosinase Inhibitors as Antibrowning Agents: An Update. Compr Rev Food Sci Food Saf (2012);11:378–98. https://doi.org/10.1111/j.1541-4337.2012.00191.x.
4. Zolghadri S, Bahrami A, Hassan Khan MT, Munoz-Munoz J, Garcia-Molina F, Garcia-Canovas F, et al. A comprehensive review on tyrosinase inhibitors. J Enzyme Inhib Med Chem (2019);34:279–309. https://doi.org/10.1080/14756366.2018.1545767.
5. Kim Y-J, Uyama H. Tyrosinase inhibitors from natural and synthetic sources: structure, inhibition mechanism and perspective for the future. Cell Mol Life Sci (2005);62:1707–23. https://doi.org/10.1007/s00018-005-5054-y.
6. Baurin N, Arnoult E, Scior T, Do QT, Bernard P. Preliminary screening of some tropical plants for anti-tyrosinase activity. J Ethnopharmacol. (2002);82(2-3):155-8. doi: 10.1016/s0378-8741(02)00174-5. PMID: 12241990.
7. Puspaningtyas AR. Evaluation of the effect of red guava (*Psidium guajava*) fruit extract on tyrosinase (EC 1.14.18.1) activity by spectrophotometry. Int Curr Pharm J (2012);1:92–7. https://doi.org/10.3329/icpj.v1i5.10280.
8. Hasegawa T. Tyrosinase-Expressing Neuronal Cell Line as *In Vitro* Model of Parkinson's Disease. Int J Mol Sci (2010);11:1082–9. https://doi.org/10.3390/ijms11031082.
9. Fernandes MS, Kerkar S. Microorganisms as a source of tyrosinase inhibitors: a review. Ann Microbiol (2017);67:343–58. https://doi.org/10.1007/s13213-017-1261-7.
10. He M, Zhang J, Li N, Chen L, He Y, Peng Z, et al. Synthesis, anti-browning effect and mechanism research of kojic acid-coumarin derivatives as anti-tyrosinase inhibitors. Food Chem X (2024);21:101128. https://doi.org/10.1016/j.fochx.2024.101128.
11. Hashemi SM, Department of Medicinal Chemistry and Pharmaceutical Sciences Research Center, Kojic acid-derived tyrosinase inhibitors: synthesis and bioactivity. Pharm Biomed Res (2015);1:1–17. https://doi.org/10.18869/acadpub.pbr.1.1.1.
12. Lee YS, Park JH, Kim MH, Seo SH, Kim HJ. Synthesis of Tyrosinase Inhibitory Kojic Acid Derivative. Arch Pharm (Weinheim) (2006);339:111–4. https://doi.org/10.1002/ardp.200500213.

13. Kim H, Choi J, Cho JK, Kim SY, Lee Y-S. Solid-phase synthesis of kojic acid-tripeptides and their tyrosinase inhibitory activity, storage stability, and toxicity. Bioorg Med Chem Lett (2004);14:2843–6. https://doi.org/10.1016/j.bmcl.2004.03.046.

14. Rezapour Niri D, Sayahi MH, Behrouz S, Moazzam A, Rasekh F, Tanideh N, et al. Design, synthesis, *in vitro*, and *in silico* evaluations of kojic acid derivatives linked to amino pyridine moiety as potent tyrosinase inhibitors. Heliyon (2023);9:e22009. https://doi.org/10.1016/j.heliyon.2023.e22009.

15. Noh J-M, Kwak S-Y, Seo H-S, Seo J-H, Kim B-G, Lee Y-S. Kojic acid–amino acid conjugates as tyrosinase inhibitors. Bioorg Med Chem Lett (2009);19:5586–9. https://doi.org/10.1016/j.bmcl.2009.08.041.

16. Peng Z, Wang G, He Y, Wang JJ, Zhao Y. Tyrosinase inhibitory mechanism and anti-browning properties of novel kojic acid derivatives bearing aromatic aldehyde moiety. Curr Res Food Sci (2023);6:100421. https://doi.org/10.1016/j.crfs.2022.100421.

17. Wang G, He M, Huang Y, Peng Z. Synthesis and biological evaluation of new kojic acid-1,3,4-oxadiazole hybrids as tyrosinase inhibitors and their application in the anti-browning of fresh-cut mushrooms. Food Chem (2023);409:135275. https://doi.org/10.1016/j.foodchem.2022.135275.

18. Shao L-L, Wang X-L, Chen K, Dong X-W, Kong L-M, Zhao D-Y, et al. Novel hydroxypyridinone derivatives containing an oxime ether moiety: Synthesis, inhibition on mushroom tyrosinase and application in anti-browning of fresh-cut apples. Food Chem (2018);242:174–81. https://doi.org/10.1016/j.foodchem.2017.09.054.

19. Hussain MI, Syed QA, Khattak MNK, Hafez B, Reigosa MJ, El-Keblawy A. Natural product coumarins: biological and pharmacological perspectives. Biologia (Bratisl) (2019);74:863–88. https://doi.org/10.2478/s11756-019-00242-x.

20. Rocchitta G, Rozzo C, Pisano M, Fabbri D, Dettori MA, Ruzza P, et al. Inhibitory Effect of Curcumin-Inspired Derivatives on Tyrosinase Activity and Melanogenesis. Molecules (2022);27:7942. https://doi.org/10.3390/molecules27227942.

21. Zou X, Yan L, Luo X, Wang E, Zhang M, Huang W, et al. Simultaneous Determination of nicotinamide, kojic acid, Tranexamic acid, raspberry glycoside, azelaic acid, magnesium ascorbate phosphate and *β*-Arbutin in whitening cosmetics by UPLC-MS/MS. MATEC Web Conf (2023);380:01005. https://doi.org/10.1051/matecconf/202338001005.

22. Wang Z, Xiang H, Dong P, Zhang T, Lu C, Jin T, et al. Pegylated azelaic acid: Synthesis, tyrosinase inhibitory activity, antibacterial activity and cytotoxic studies. J Mol Struct (2021);1224:129234. https://doi.org/10.1016/j.molstruc.2020.129234.

23. Sauer N, Oślizło M, Brzostek M, Wolska J, Lubaszka K, Karłowicz-Bodalska K. The multiple uses of azelaic acid in dermatology: mechanism of action, preparations, and potential therapeutic applications. Adv Dermatol Allergol (2024);40:716–24. https://doi.org/10.5114/ada.2023.133955.

24. Xu H, Li X, Mo L, Zou Y, Zhao G. Tyrosinase inhibitory mechanism and the anti-browning properties of piceid and its ester. Food Chem (2022);390:133207. https://doi.org/10.1016/j.foodchem.2022.133207.

25. Vaezi M. Structure and inhibition mechanism of some synthetic compounds and phenolic derivatives as tyrosinase inhibitors: review and new insight. J Biomol Struct Dyn (2023);41:4798–810. https://doi.org/10.1080/07391102.2022.2069157.

26. Tomczyk M,Oxidation of flavonoids by tyrosinase and by o-quinones–comment on Flavonoids as tyrosinase inhibitors in *in silico* and *in vitro* models: basic framework of SAR using a statistical modelling approach. J Enzyme Inhib Med Chem (2022);37:427-436. https://doi.org/10.1080/14756366.2023.2269613.

27. Farasat A, Ghorbani M, Gheib N, Shariatifar H. *In silico* assessment of the inhibitory effect of four flavonoids (Chrysin, Naringin, Quercetin, Kaempferol) on tyrosinase activity using the MD simulation approach. BioTechnologia (2020);101:193–204. https://doi.org/10.5114/bta.2020.97878.

28. Chen J, Zhang Z, Li H, Tang H. Exploring the effect of a series of flavonoids on tyrosinase using integrated enzyme kinetics, multispectroscopic, and molecular modelling analyses. Int J Biol Macromol (2023);252:126451. https://doi.org/10.1016/j.ijbiomac.2023.126451.

29. Obaid RJ, Mughal EU, Naeem N, Sadiq A, Alsantali RI, Jassas RS, et al. Natural and synthetic flavonoid derivatives as new potential tyrosinase inhibitors: a systematic review. RSC Adv (2021);11:22159–98. https://doi.org/10.1039/D1RA03196A.

30. Zhu L, Lu Y, Yu W-G, Zhao X, Lu Y-H. Anti-photoageing and anti-melanogenesis activities of chrysin. Pharm Biol (2016);54:2692–700. https://doi.org/10.1080/13880209.2016.1179334.

31. Zhang C, Lu Y, Tao L, Tao X, Su X, Wei D. Tyrosinase inhibitory effects and inhibition mechanisms of nobiletin and hesperidin from citrus peel crude extracts. J Enzyme Inhib Med Chem 2007;22:83–90. https://doi.org/10.1080/14756360600953876.

32. Fan M, Zhang G, Hu X, Xu X, Gong D. Quercetin as a tyrosinase inhibitor: Inhibitory activity, conformational change and mechanism. Food Res Int (2017);100:226–33. https://doi.org/10.1016/j.foodres.2017.07.010.

33. Rho HS, Ghimeray AK, Yoo DS, Ahn SM, Kwon SS, Lee KH, et al. Kaempferol and Kaempferol Rhamnosides with Depigmenting and Anti-Inflammatory Properties. Molecules (2011);16:3338–44. https://doi.org/10.3390/molecules16043338.

34. Şöhretoğlu D, Sari S, Barut B, Özel A. Tyrosinase inhibition by some flavonoids: Inhibitory activity, mechanism by *in vitro* and *in silico* studies. Bioorganic Chem (2018);81:168–74. https://doi.org/10.1016/j.bioorg.2018.08.020.

35. Boo YC. Arbutin as a Skin Depigmenting Agent with Antimelanogenic and Antioxidant Properties. Antioxidants (2021);10:1129. https://doi.org/10.3390/antiox10071129.

36. Siridechakorn I, Pimpa J, Choodej S, Ngamrojanavanich N, Pudhom K. Synergistic impact of arbutin and kaempferol-7-O-α-l-rhamnopyranoside from *Nephelium lappaceum* L. on whitening efficacy and stability of cosmetic formulations. Sci Rep (2023);13:22004. https://doi.org/10.1038/s41598-023-49351-3.

37. Masyita A, Rifai Y. Molecular Docking Studies of Arbutin Derivatives as Tyrosinase Inhibitors. Int J Biosci Biochem Bioinforma (2019);9:188–93. https://doi.org/10.17706/ijbbb.2019.9.3.188-193.

38. Yang C-H, Chen Y-S, Lai J-S, Hong WWL, Lin C-C. Determination of the Thermodegradation of deoxyArbutin in Aqueous Solution by High Performance Liquid Chromatography. Int J Mol Sci (2010);11:3977–87. https://doi.org/10.3390/ijms11103977.

39. Xie D, Fu W, Yuan T, Han K, Lv Y, Wang Q, et al. 6′-O-Caffeoylarbutin from Quezui Tea: A Highly Effective and Safe Tyrosinase Inhibitor. Int J Mol Sci (2024);25:972. https://doi.org/10.3390/ijms25020972.

40. Chang N-F, Chen Y-S, Lin Y-J, Tai T-H, Chen A-N, Huang C-H, et al. Study of Hydroquinone Mediated Cytotoxicity and Hypopigmentation Effects from UVB-Irradiated Arbutin and DeoxyArbutin. Int J Mol Sci (2017);18:969. https://doi.org/10.3390/ijms18050969.

41. Hamed SH, Sriwiriyanont P, deLong MA, Visscher MO, Wickett RR, Boissy RE. Comparative efficacy and safety of deoxyarbutin, a new tyrosinase-inhibiting agent. J Cosmet Sci. (2006) Jul-Aug;57(4):291-308. PMID: 16957809.

42. Migas P, Krauze-Baranowska M. The significance of arbutin and its derivatives in therapy and cosmetics. Phytochem Lett (2015);13:35–40. https://doi.org/10.1016/j.phytol.2015.05.015.

43. Hong J-H, Chen H-J, Xiang S-J, Cao S-W, An B-C, Ruan S-F, et al. Capsaicin reverses the inhibitory effect of licochalcone α/β-Arbutin on tyrosinase expression in b16 mouse melanoma cells. Pharmacogn Mag (2018);14:110. https://doi.org/10.4103/pm.pm_103_17.

44. Jiang L, Wang D, Zhang Y, Li J, Wu Z, Wang Z, et al. Investigation of the pro-apoptotic effects of arbutin and its acetylated derivative on murine melanoma cells. Int J Mol Med (2017). https://doi.org/10.3892/ijmm.2017.3256.

45. Wang W, Gao Y, Wang W, Zhang J, Yin J, Le T, et al. Kojic Acid Showed Consistent Inhibitory Activity on Tyrosinase from Mushroom and in Cultured B16F10 Cells Compared with Arbutins. Antioxidants (2022);11:502. https://doi.org/10.3390/antiox11030502.

46. Chen Y-R, Chiou RY-Y, Lin T-Y, Huang C-P, Tang W-C, Chen S-T, et al. Identification of an Alkylhydroquinone from Rhus succedanea as an Inhibitor of Tyrosinase and Melanogenesis. J Agric Food Chem (2009);57:2200–5. https://doi.org/10.1021/jf802617a.

47. Sudhesh Dev S, Zainal Abidin SA, Farghadani R, Othman I, Naidu R. Receptor Tyrosine Kinases and Their Signaling Pathways as Therapeutic Targets of Curcumin in Cancer. Front Pharmacol (2021);12:772510. https://doi.org/10.3389/fphar.2021.772510.

48. Susilawati Y, Chaerunisa A, Purwaningsih H. Phytosome drug delivery system for natural cosmeceutical compounds: Whitening agent and skin antioxidant agent. J Adv Pharm Technol Res (2021);12:327. https://doi.org/10.4103/japtr.JAPTR_100_20.

49. Huang H-C, Chiu S-H, Chang T-M. Inhibitory Effect of [6]-Gingerol on Melanogenesis in B16F10 Melanoma Cells and a Possible Mechanism of Action. Biosci Biotechnol Biochem (2011);75:1067–72. https://doi.org/10.1271/bbb.100851.

50. Shen Y, Song X, Li L, Sun J, Jaiswal Y, Huang J, et al. Protective effects of p-coumaric acid against oxidant and hyperlipidemia-an *in vitro* and *in vivo* evaluation. Biomed Pharmacother (2019);111:579–87. https://doi.org/10.1016/j.biopha.2018.12.074.

51. Masek A, Chrzescijanska E, Latos M. Determination of Antioxidant Activity of Caffeic Acid and p-coumaric Acid by Using Electrochemical and Spectrophotometric Assays. Int J Electrochem Sci (2016);11:10644–58. https://doi.org/10.20964/2016.12.73.

52. Oliveira L, Ferrarini M, Dos Santos AP, Varela MT, Corrêa ITS, Tempone AG, et al. Coumaric acid analogues inhibit growth and melanin biosynthesis in *Cryptococcus neoformans* and potentialize amphotericin B antifungal activity. Eur J Pharm Sci (2020);153:105473. https://doi.org/10.1016/j.ejps.2020.105473.

53. Boo YC. *p*-Coumaric Acid as An Active Ingredient in Cosmetics: A Review Focusing on its Antimelanogenic Effects. Antioxidants (2019);8:275. https://doi.org/10.3390/antiox8080275.

54. Cho J-G, Huh J, Jeong R-H, Cha B-J, Shrestha S, Lee D-G, et al. Inhibition effect of phenyl compounds from the *Oryza sativa* roots on melanin production in murine B16-F10 melanoma cells. Nat Prod Res (2015);29:1052–4. https://doi.org/10.1080/14786419.2014.968155.

55. Goenka S, Johnson F, Simon SR. Novel Chemically Modified Curcumin (CMC) Derivatives Inhibit Tyrosinase Activity and Melanin Synthesis in B16F10 Mouse Melanoma Cells. Biomolecules (2021);11:674. https://doi.org/10.3390/biom11050674.

56. Chiriapkin A, Kodonidi I, Pozdnyakov D. Targeted Synthesis and Study of Anti-tyrosinase Activity of 2-Substituted Tetrahydrobenzo[4,5]Thieno[2,3-d] Pyrimidine-4(3H)-One. Iran J Pharm Res (2022);21. https://doi.org/10.5812/ijpr-126557.

57. Safithri M, Andrianto D, Gaisani Arda A, Hawa Syaifie P, Mardia Ningsih Kaswati N, Mardliyati E, et al. The effect of red betel (*Piper crocatum*) water fraction as tyrosinase inhibitors: *In vitro*, molecular docking, and molecular dynamics studies. J King Saud Univ Sci (2023);35:102933. https://doi.org/10.1016/j.jksus.2023.102933.

58. Song Y, Li J, Tian H, Xiang H, Chen S, Li L, et al. Copper chelating peptides derived from tilapia (*Oreochromis niloticus*) skin as tyrosinase inhibitor: Biological evaluation, *in silico* investigation and *in vivo* effects. Food Res Int (2023);163:112307. https://doi.org/10.1016/j.foodres.2022.112307.

59. Bernard, Berthon. Resveratrol: an original mechanism on tyrosinase inhibition. Int J Cosmet Sci (2000);22:219–26. https://doi.org/10.1046/j.1467-2494.2000.00019.x.

60. Liu Q, Kim C, Jo Y, Kim S, Hwang B, Lee M. Synthesis and Biological Evaluation of Resveratrol Derivatives as Melanogenesis Inhibitors. Molecules (2015);20:16933–45. https://doi.org/10.3390/molecules200916933.

61. Zimmermann Franco DC, Gonçalves De Carvalho GS, Rocha PR, Da Silva Teixeira R, Da Silva AD, Barbosa Raposo NR. Inhibitory Effects of Resveratrol Analogs on Mushroom Tyrosinase Activity. Molecules (2012);17:11816–25. https://doi.org/10.3390/molecules171011816.

62. Tanaka H, Nishimaki-Mogami T, Tamehiro N, Shibata N, Mandai H, Ito S, et al. Pterostilbene, a Dimethyl Derivative of Resveratrol, Exerts Cytotoxic Effects on Melanin-Producing Cells through Metabolic Activation by Tyrosinase. Int J Mol Sci (2024);25:9990. https://doi.org/10.3390/ijms25189990.

63. Zeng H-J, Li Q-Y, Ma J, Yang R, Qu L-B. A comparative study on the effects of resveratrol and oxyresveratrol against tyrosinase activity and their inhibitory mechanism. Spectrochim Acta A Mol Biomol Spectrosc (2021);251:119405. https://doi.org/10.1016/j.saa.2020.119405.

64. Pal R, Teli G, Matada GSP, Dhiwar PS. Designing strategies, structural activity relationship and biological activity of recently developed nitrogen containing heterocyclic compounds as epidermal growth factor receptor tyrosinase inhibitors. J Mol Struct (2023);1291:136021. https://doi.org/10.1016/j.molstruc.2023.136021.

65. Butt ARS, Abbasi MA, Aziz-ur-Rehman, Siddiqui SZ, Raza H, Hassan M, et al. Synthesis and structure-activity relationship of tyrosinase inhibiting novel bi-heterocyclic acetamides: Mechanistic insights through enzyme inhibition, kinetics and computational studies. Bioorganic Chem (2019);86:459–72. https://doi.org/10.1016/j.bioorg.2019.01.036.

66. Havasi MH, Ressler AJ, Parks EL, Cocolas AH, Weaver A, Seeram NP, et al. Antioxidant and tyrosinase docking studies of heterocyclic sulfide derivatives containing a thymol moiety. Inorganica Chim Acta (2020);505:119495. https://doi.org/10.1016/j.ica.2020.119495.

67. Peng Z, Wang G, Zeng Q-H, Li Y, Liu H, Wang JJ, et al. A systematic review of synthetic tyrosinase inhibitors and their structure-activity relationship. Crit Rev Food Sci Nutr (2022);62:4053–94. https://doi.org/10.1080/10408398.2021.1871724.

68. Ghani U. Azole inhibitors of mushroom and human tyrosinases: Current advances and prospects of drug development for melanogenic dermatological disorders. Eur J Med Chem (2022);239:114525. https://doi.org/10.1016/j.ejmech.2022.114525.

69. Hassan M, Shahzadi S, Kloczkowski A. Tyrosinase Inhibitors Naturally Present in Plants and Synthetic Modifications of These Natural Products as Anti-Melanogenic Agents: A Review. Molecules (2023);28:378. https://doi.org/10.3390/molecules28010378.

70. Mughal EU, Ashraf J, Hussein EM, Nazir Y, Alwuthaynani AS, Naeem N, et al. Design, Synthesis, and Structural Characterization of Thioflavones and Thioflavonols as Potential Tyrosinase Inhibitors: *In Vitro* and *In Silico* Studies. ACS Omega (2022);7:17444–61. https://doi.org/10.1021/acsomega.2c01841.

71. Mermer A, Demirci S. Recent advances in triazoles as tyrosinase inhibitors. Eur J Med Chem (2023);259:115655. https://doi.org/10.1016/j.ejmech.2023.115655.

72. Shakila S, Abbasi MA, Rehman A-, Siddiqui SZ, Nazir M, Muhammad S, et al. Convergent Synthesis, Kinetics and Computational Comprehensions of Indole- (Phenyl) triazole Bi-heterocycles Amalgamated with Propanamides as Elastase Inhibitors (2024). https://doi.org/10.21203/rs.3.rs-4361622/v1.

ANADOLU UNIVERSITY
FACULTY OF PHARMACY

European Journal of Life Sciences 2024; 3: 127-135

Review Article

The blood-brain barrier: a focus on neurovascular unit components

Betül Can[1], İbrahim Özkan Alataş[1]

[1]Eskişehir Osmangazi University, Faculty of Medicine, Department of Medical Biochemistry, Eskişehir, Türkiye.

✉ Betül Can
betul_cn@yahoo.com

https://doi.org/10.55971/EJLS.1533200

Received: 14.08.2024
Accepted: 17.12.2024
Available online: 31.12.2024

ABSTRACT

The blood–brain barrier (BBB) provides an optimum environment for neurons by ensuring the integrity and homeostasis of highly fragile brain cells under physiological conditions, protecting the brain from changes in the blood with both structural (tight junctions) and metabolic (enzymes) barriers, selective transport, and the metabolism and modification of substances in the blood and brain. The endothelial cells of the brain capillaries, located at the interfaces between the blood and the brain, are critical components that limit the permeability of the BBB. These cells have unique morphological, biochemical, and functional characteristics that distinguish them from those found in the peripheral vascular system. In addition to endothelial cells, astrocytic perivascular end-feet, pericytes, neurons, microglia, and smooth muscle cells also play significant roles in maintaining the homeostasis of the brain parenchyma. Thus, the BBB effectively prevents various molecules and therapeutic drugs from entering the brain parenchyma and reaching the target area at sufficiently high concentrations. The passage of a substance through the BBB and its entry into the brain depends on various factors, including the substance's lipophilicity, diffusion capability, molecular weight, electrical charge, blood concentration, and multiple primary and secondary factors. Drug delivery systems developed in recent years, through techniques and methods aimed at controlled and safe opening or bypassing of the BBB, are believed to provide significant benefits in the lesion area by allowing therapeutic substances to optimally enter the brain from the circulation. This article provides a review of the BBB and its components, highlighting their significance among the brain's different interfaces. It also discusses approaches for delivering therapeutic substances to the affected area under optimal conditions and concentrations in various brain pathologies.

Keywords: Astrocytic perivascular end-feet, blood-brain barrier, drug delivery, microglia, neurovascular unit

1. INTRODUCTION

In the central nervous system (CNS), neurons communicate through chemical and electrical signals. Therefore, for healthy neural signaling, precise regulation in the local ionic microenvironment of synapses and axons is essential [1]. During the regulation of molecular exchanges between blood, neural tissue, and the fluid-filled spaces within the brain, six interfaces play a role: the blood–brain barrier (BBB), the blood–cerebrospinal fluid (CSF) barrier, the meningeal barrier, the circumventricular organs, the adult brain ependyma, and the fetal neuroependyma [2]. In this review, various concepts related to the BBB, the prominent features and functions of the components constituting the BBB,

the transport systems involved in crossing the BBB, the limitation of drug passage into the brain due to the BBB's strong barrier properties in various brain diseases, and various invasive and noninvasive strategies developed to overcome this barrier and enhance therapeutic efficacy are examined.

2. COMPONENTS AND FEATURES OF THE BBB

The BBB is a dynamic interface that separates the brain interstitium from the luminal contents of the cerebral vascular system [3]. This interface maintains the integrity of highly fragile brain cells under physiological conditions, ensures brain homeostasis, and provides an optimal environment by protecting the CNS from various physiological and pathological changes. Instead of the commonly used term "Blood–Brain Barrier," some researchers in recent years have proposed the concept of "Blood–Brain Border" [4].

The neurovascular unit (NVU) is a complex functional unit that reflects the dynamic communication between the components of the BBB and neurons [5]. It is composed of microvascular endothelial cells surrounded by a basal lamina, astrocytic perivascular end-feet, pericytes, neurons, microglia, and smooth muscle cells [6,3]. Below is a brief overview of the components that make up the NVU and maintain the integrity of the BBB.

2.1. Endothelial cells

Microvascular endothelial cells are considered the anatomical foundation of the BBB due to their distinctive morphological, biochemical, and functional characteristics that set them apart from their counterparts in the peripheral vascular system [7,8]. These cells, which line the inner surface of brain capillaries in a single layer and are in direct contact with the blood, are characterized by being surrounded by the basal lamina and astrocytic perivascular end-feet, containing tight junctions (TJs) composed of transmembrane proteins such as claudin, occludin, and junction adhesion molecules, having very few pinocytic vesicles in their cytoplasm, and lacking fenestrations [9,10]. In addition, these cells have smooth, oval nuclei with irregularly distributed chromatin, caveolae, similar invaginations on the luminal side, and large quantities of mitochondria to enhance energy potential for enzyme and transport system activities. They are also equipped with specialized transport systems and receptors that facilitate the uptake of nutrients and hormones essential for brain function [8].

To eliminate gaps between endothelial cells and prevent the paracellular diffusion of substances from the blood into the brain parenchymal area, the endothelial cells of capillaries and postcapillary venules not only possess TJs, which provide primary isolation but also have adherens junctions. These junctions restrict the paracellular flow of hydrophilic molecules but do not limit the passage of small lipophilic molecules such as O_2 and CO_2. Thus, these molecules can diffuse freely across plasma membranes along concentration gradients. The diffusion of O_2 and CO_2 across the endothelium is emphasized as being essential for regulating brain metabolism and pH in NVU cells [11].

The BBB not only functions as a physical barrier but also acts as a metabolic (enzymatic) barrier due to the expression of numerous enzymes by endothelial cells that can modify a variety of molecules. These enzymes can either inactivate pharmacologically active drugs or activate inactive prodrugs [12]. These include L-amino acid decarboxylase, monoamine oxidase, glutamyl aminopeptidase, transaminases, and especially cytochrome p450 enzymes. It has been noted that some molecules with neuroactivity, such as neurotransmitters or drugs that could affect normal physiological brain functions are prevented from entering the brain by being enzymatically converted into inactive forms once they penetrate from the luminal surface of the capillary endothelium into the cytoplasm [13].

2.2. Basement membrane

The blood vessels of the CNS contain various basement membranes, including endothelial, astroglial, and meningeal. The astroglial and leptomeningeal basement membranes form the parenchymal basement membrane that defines the boundary of the brain parenchyma. In brain capillaries, the endothelial and parenchymal basement

membranes merge to form a single basement membrane [7]. The basement membrane, structured by brain microvascular endothelial cells, pericytes, and astrocytes, is made up of three adjacent layers composed of various extracellular matrix molecule classes, including collagen, elastin, fibronectin, laminin, and proteoglycans [14]. Thus, the brain endothelium is supported by the extracellular matrix and basement membranes, along with other cells of the NVU [15]. Although the basement membrane does not constitute an important barrier against the diffusion of small molecules, it has been emphasized that it plays key roles in anchoring cells and regulating the functions of endothelial cells through various signaling molecules [16]. The basement membrane can become thicker or thinner in response to stress stimuli and certain pathological conditions. The loss of the characteristic features of the basement membrane is considered one of the factors leading to the disruption of the BBB structure [8].

2.3. Astrocytes

Astrocytes are specialized glial cells with crucial roles in the CNS. Their end-feet cover the basal membrane on the outer surface of the BBB endothelium. They are characterized by numerous extensions containing intermediate filaments of the cell cytoskeleton and glial fibrillary acidic protein. These cells cover more than 99% of the abluminal surface of cerebral vessels [17] and contribute to the structure, development, and unique endothelial phenotype of the BBB. Their roles are thought to be facilitated by their anatomical proximity to endothelial cells and the expression and release of soluble factors [8]. The parenchymal surface of cerebral vessels is completely covered by a mosaic of astrocytic end-feet and separated by gaps of approximately 20 μm [3]. Astrocytes interacting with endothelial cells strengthen TJs and reduce the gap junction area, playing a crucial role in the limited permeability and integrity of the BBB. A study investigating the importance of astrocytes in the induction of BBB properties suggested that astrocytes interacting with endothelial cells increase transendothelial electrical resistance and that the proximity of astrocytes to the endothelium is effective in the development of a tight BBB [18]. Due to their polarized anatomical structure and the proximity of their end-feet to smooth muscle cells in arterioles and pericytes, astrocytes are also noted to play a role in regulating blood flow during neuronal activity [19]. Astrocytes contribute to various functions, including synapse formation and plasticity, energetic and redox metabolism, and synaptic homeostasis of ions and neurotransmitters like glutamate. They regulate cerebral blood flow in response to local neuronal activity changes by not only stimulating vascular smooth muscle cells but also by modulating these diverse functions [20]. Therefore, astrocytes are recognized as central to dynamic signaling within the NVU and play a significant role in coordinating neurovascular coupling [21].

2.4. Pericytes

Brain pericytes are polymorphic cells with a spherical or oval cell body and a distinct round nucleus. They also have long cytoplasmic processes with heterogeneous morphology that are positioned along the axis of the blood vessel [22], as well as secondary and tertiary processes that encircle the vascular wall with smaller, circular branches [8]. Pericytes, which contribute to the regulation of cerebral blood flow and strengthen the BBB's impermeability, are embedded in the endothelial basement membrane at varying intervals along the vessel [3]. Pericytes contain various proteins, including contractile proteins, cytoskeletal components, and surface antigens. The predominant contractile protein localized in microfilament bundles is smooth muscle actin [8]. However, their morphology and protein expression can vary along the microvascular tree [23]. Additionally, pericytes can differentiate into fibroblasts, smooth muscle cells, macrophages, and other cell populations [24]. It has also been reported that adult CNS microvascular pericytes possess neural cell potential and serve as a source of multipotential progenitor cells [25]. Significant findings indicate that pericytes can regulate blood flow in response to neuronal activity, whereas capillary diameter does not change in regions lacking pericytes. This suggests that pericytes, rather than endothelial cells, play a role in capillary diameter changes due to their possession of contractile proteins [26]. In

larger vessels, it is emphasized that myocytes are the primary effectors of changes in vessel diameter within the NVU [27]. A study investigating the *in vivo* roles of pericytes in the BBB found that pericytes regulate BBB-specific gene expression in endothelial cells, induce the polarization of astrocytic end-feet, and that the extent of pericyte coverage of capillaries is significantly related to the integrity, permeability, and regulation of the BBB [28].

Due to their subendothelial location in the microvascular structure, it has been suggested that pericytes may also play a role in regulating coagulation events that occur following cerebrovascular lesion formation [29]. It has been suggested that pericytes negatively regulate fibrinolysis in brain endothelial cells in vitro, thereby supporting procoagulant activity. Additionally, pericytes may exhibit endogenous anticoagulant activity due to their role as a major *in vitro* source of the serpin protease nexin-1, known for its antithrombin effects [30]. Therefore, pericytes, which are important components of the NVU, play an essential role in the local coagulation process due to their pro- and anti-coagulant effects.

2.5. Microglia

Microglia are a type of glial cell with immune-competent and phagocytic properties in the CNS [31], constituting approximately 10%–15% of all glial cells [32]. They are derived from myeloid progenitors in the embryonic yolk sac and proliferate to colonize the entire parenchyma after migrating to the developing neural tube [33]. They continuously monitor the brain parenchyma and play a crucial role in maintaining the homeostasis of nervous tissue [34].

Microglia are primarily characterized by two fundamental morphologies, depending on the physiological and pathological conditions in the brain. Under physiological conditions, resting microglia have slender, elongated processes that give them a branched morphology. These processes allow the cells to promptly detect homeostatic disturbances in the CNS [31]. These microglia are characterized by a small cell body (5–10 μm) and exhibit minimal or no cellular movement [35]. Their processes are constantly in motion, extending outward from the cell body to survey large areas, protruding and retracting to interact with NVU components such as neurons, astrocytes, and blood vessels. This allows them to continuously monitor the functional status of synapses [33]. A recent study has found that near the tips of the long processes of microglia, there are actin-dependent, thin, hair-like filopodia that can extend and retract more quickly than the main processes. These filopodia significantly increase the effective sensing volume of microglia [36]. During a pathological condition (such as trauma or inflammatory stimuli), microglia rapidly become activated, transforming into a phagocytic morphology characterized by a large cell body and short processes. This transformation is related to the type and severity of the damage [35] and is associated with changes in the release of cytotoxic substances such as oxygen radicals, proteases, and proinflammatory cytokines, as well as alterations in surface antigens [31]. Microglial reactivity under pathological conditions is complex, as these cells can exhibit different phenotypes over time or even simultaneously. Although the mechanism underlying these phenotype differences is not clear, reactive microglia are classified as M1 (proinflammatory and neurotoxic) and M2 (anti-inflammatory and neuroprotective) [37]. M1 microglia are notable for their proinflammatory and prokilling functions, while M2 microglia play roles in immune regulation and repair. Additionally, the phagocytic ability of M2 microglia reveals their capacity to clear cellular debris and contribute to neural repair [35]. It has been reported that activated microglia can provide immune optimization by interacting and cooperating with astrocytes, another important component of the NVU, in conditions such as neuroinflammation [38].

3. DRUG DELIVERY AND BBB OPENING APPROACHES

3.1. Challenges for drug delivery

The passage of certain substances through the BBB and their entry into the brain depends on numerous primary and secondary factors. These factors include the size of the molecule, its flexibility, conformation, ionization, charge, hydrophilic/lipophilic properties, the number of hydrogen bond donors/acceptors,

cellular enzyme secretion/stability, affinity for efflux mechanisms, and affinity for carrier mechanisms [39]. In addition, systemic enzymatic stability, affinity for plasma protein binders, uptake of the drug into non-target tissues, clearance rate, cerebral blood flow, diet, age, gender, species, and the effects of existing pathological conditions are also considered important peripheral factors [40]. It has been reported that more than 98% of large pharmaceuticals with different structures such as peptides and proteins, and even all small molecules, can not pass the BBB [41]. Theoretically, it is emphasized that for a molecule to cross the BBB in pharmacologically significant amounts, its molecular weight should be <400 Da, the molecule should be lipid soluble and should not be a substrate for an active efflux transporter at the BBB [42]. It should be also taken into account that lipophilic molecules, even if they are <400 Da, can be degraded by specific enzymes expressed by BBB cells and thus be trapped in the metabolic barrier [43].

The early stages of drug discovery studies, especially based on the design of orally applicable molecules, are guided by Lipinski's "rule of five" (Ro5), which is an experimental and computational approach related to the solubility and permeability of the molecule [44]. This rule is actually related to the four physicochemical properties of a molecule, namely its molecular weight, lipophilicity, and the number of hydrogen bond donors or acceptors, and is named after the cutoff points of each parameter being close to 5 or a multiple of 5. According to this rule, it is reported that poor absorption or permeability, i.e. less oral bioavailability, is more likely in the following cases: i) molecular weight >500, ii) calculated Log P (CLogP) value is above 5 (partition coefficient, P, value is parallel to the hydrophobicity of the molecule), iii) more than 5 hydrogen bond donors, and iv) more than 10 hydrogen bond acceptors [45]. Today, the Ro5 rule is still used in brain studies which are based on drug design, synthesis, and oral bioavailability [46].

For assessing BBB passage, the concentrations of therapeutic drugs in the blood and pharmacokinetic calculations need to be considered. These calculations utilize the equation [%ID/g = PS × AUC] [43,12]. In this equation, "%ID/g" is the percent injected dose per gram of brain, "PS" is the brain permeability surface area, and "AUC" is the steady-state area under the plasma concentration curve [47]. Accordingly, it is noted that drug uptake by the brain can be increased through stabilizing the drug in the blood (e.g., increasing AUC) and making modifications to the drug structure to enhance passive permeability and/or specificity via transport systems. Strategies such as drug manipulation and opening/circumventing the BBB have been emphasized for this purpose [12]. Similarly, it has been suggested that transiently increasing BBB permeability in a controlled and safe manner through various methods could enable higher drug concentrations to reach brain tissue from the bloodstream, potentially offering hope for treating localized malignant diseases in the brain [48].

3.2. Invasive and non-invasive strategies

Various mechanisms are involved in the passage of substances through the BBB. These mechanisms include paracellular diffusion, transcellular diffusion, carrier-mediated transport, receptor-mediated transport, absorptive-mediated transport, and cell-mediated transport. Additionally, the efficacy of efflux transporters in removing harmful substances that reach the CNS is also emphasized [49]. Mechanical damage (trauma, surgical operations), ischemia (reduced/blocked blood flow), infiltration of immune cells (inflammation), activation of matrix metalloproteinases, increase in reactive oxygen species (oxidative stress), chemicals (exposure to heavy metals, pesticides), radiation, and some biological factors can lead to disruption of BBB integrity [50]. It is known that some primary brain tumors also damage the BBB and increase its permeability; however, this is a limited increase, and these malignancies are protected from therapeutic agents due to the intact blood–tumor barrier in peritumoral regions [51]. For these reasons, there is an important need to develop new drugs to cope with various pathologies affecting the central nervous system, and various strategies are being followed to overcome the problem of these drugs not being able to cross the BBB. In these studies, various invasive and noninvasive methods have been employed. Invasive methods include direct injection of drugs into the brain parenchyma for therapeutic purposes,

manipulation of certain hyperosmolar solutions [52], implantation of controlled release systems [53], and focused ultrasound using microbubbles [54]. Noninvasive methods include the nose-to-brain pathway, inhibition of efflux transporters, chemical modification of drugs, and the use of nanocarriers (such as liposomes, lipid/polymeric/inorganic nanoparticles, nanogels, and nanoemulsions) [49]. The intracranial drug delivery, one of the invasive methods, has been considered as an interesting treatment strategy compared to systemic application in difficult-to-treat epilepsies. Although this method has some advantages, such as giving the opportunity to use substances that are impermeable to the BBB, reducing the risk of systemic/neurological side effects, and reaching high drug concentrations in the targeted localization, and some disadvantages such as being an invasive procedure and difficulty in long-term administration of the drug have been reported [55]. The nose-to-brain route, one of the non-invasive methods, not only increases the brain bioavailability of the drug by reaching the central nervous system directly through the olfactory and trigeminal nerve pathways, but also it is a promising route even in aggressive brain cancer such as glioblastoma due to the high vascularization of the nasal mucosa, reduced systemic metabolism, low risk of infection and suitability for chronic use [56,57]. The safety, efficacy, feasibility, advantages, disadvantages, and potential complications of these approaches in clinical applications have been debated for years and continue to be a topic of ongoing discussion.

4. CONCLUSION

The BBB maintains the integrity and homeostasis of brain cells under physiological conditions by providing a physical barrier, a metabolic barrier, and selective transport systems. It protects the brain from changes in the blood, metabolizes and modifies substances in the blood and brain, and ensures an optimal environment for neurons. However, while this vital system protects the brain from potentially harmful compounds, it also presents a major barrier to the passage of therapeutic drugs into the brain parenchyma in various brain pathologies. It appears that various physicochemical properties of substances used for therapeutic purposes and some peripheral factors significantly affect BBB bioavailability. Various invasive or non-invasive strategies are being followed in order to increase the effectiveness of treatment in various brain diseases by overcoming the BBB barrier in a controlled manner. In recent years, some of the non-invasive strategies are promising even in the most aggressive brain cancers. Considering the wide spectrum of central nervous system diseases, it is clear that there is a significant need for new drug designs or formulations with pharmacokinetic profiling and the development of optimal treatment strategies.

Ethical approval

Not applicable, because this article does not contain any studies with human or animal subjects.

Author contribution

Conceptualization, B.C. and İ.Ö.A; Writing, B.C.; Supervision, İ.Ö.A. All authors have read and agreed to the published version of the manuscript.

Source of funding

This research received no grant from any funding agency/sector.

Conflict of interest

The authors declared that there is no conflict of interest.

REFERENCES

1. Abbott NJ, Patabendige AA, Dolman DE, Yusof SR, Begley DJ. Structure and function of the blood-brain barrier. Neurobiol Dis. (2010);37(1):13-25. https://doi.org/10.1016/j.nbd.2009.07.030.
2. Saunders NR, Ek CJ, Habgood MD, Dziegielewska KM. Barriers in the brain: a renaissance? Trends Neurosci. (2008);31(6):279-86. https://doi.org/10.1016/j.tins.2008.03.003

3. Stokum JA, Gerzanich V, Simard JM. Molecular pathophysiology of cerebral edema. J Cereb Blood Flow Metab. (2016);36(3):513-38. https://doi.org/10.1177/0271678X15617172

4. Badaut J, Ghersi-Egea JF, Thorne RG, Konsman JP. Blood-brain borders: a proposal to address limitations of historical blood-brain barrier terminology. Fluids Barriers CNS. (2024);21(1):3. https://doi.org/10.1186/s12987-023-00478-5

5. McConnell HL, Mishra A. Cells of the Blood-Brain Barrier: An Overview of the Neurovascular Unit in Health and Disease. Methods Mol Biol. (2022);2492:3-24. https://doi.org/10.1007/978-1-0716-2289-6_1

6. Zlokovic BV. Neurovascular pathways to neurodegeneration in Alzheimer's disease and other disorders. Nat Rev Neurosci. (2011);12(12):723-38. https://doi.org/10.1038/nrn3114

7. Engelhardt B, Sorokin L. The blood-brain and the blood-cerebrospinal fluid barriers: function and dysfunction. Semin Immunopathol. (2009);31(4):497-511. https://doi.org/10.1007/s00281-009-0177-0

8. Sá-Pereira I, Brites D, Brito MA. Neurovascular unit: a focus on pericytes. Mol Neurobiol. (2012);45(2):327-47. https://doi.org/10.1007/s12035-012-8244-2

9. Srinivasan B, Kolli AR, Esch MB, Abaci HE, Shuler ML, Hickman JJ. TEER measurement techniques for *in vitro* barrier model systems. J Lab Autom. (2015);20(2):107-26. https://doi.org/10.1177/2211068214561025

10. Hawkins BT, Davis TP. The blood-brain barrier/neurovascular unit in health and disease. Pharmacol Rev. (2005);57(2):173-85. https://doi.org/10.1124/pr.57.2.4

11. Kadry H, Noorani B, Cucullo L. A blood-brain barrier overview on structure, function, impairment, and biomarkers of integrity. Fluids Barriers CNS. (2020);17(1):69. https://doi.org/10.1186/s12987-020-00230-3

12. Koziara JM, Lockman PR, Allen DD, Mumper RJ. The blood-brain barrier and brain drug delivery. J Nanosci Nanotechnol. (2006);6(9-10):2712-35. https://doi.org/10.1166/jnn.2006.441

13. Minn A, Ghersi-Egea JF, Perrin R, Leininger B, Siest G. Drug metabolizing enzymes in the brain and cerebral microvessels. Brain Res Brain Res Rev. (1991);16(1):65-82. https://doi.org/10.1016/0165-0173(91)90020-9

14. Cardoso FL, Brites D, Brito MA. Looking at the blood-brain barrier: molecular anatomy and possible investigation approaches. Brain Res Rev. (2010);64(2):328-63. https://doi.org/10.1016/j.brainresrev.2010.05.003

15. Abbott NJ, Friedman A. Overview and introduction: the blood-brain barrier in health and disease. Epilepsia. (2012);53 Suppl 6(0 6):1-6. https://doi.org/10.1111/j.1528-1167.2012.03696.x

16. Carvey PM, Hendey B, Monahan AJ. The blood-brain barrier in neurodegenerative disease: a rhetorical perspective. J Neurochem. (2009);111(2):291-314. https://doi.org/10.1111/j.1471-4159.2009.06319.x

17. Filosa JA, Morrison HW, Iddings JA, Du W, Kim KJ. Beyond neurovascular coupling, role of astrocytes in the regulation of vascular tone. Neuroscience. (2016);323:96-109. https://doi.org/10.1016/j.neuroscience.2015.03.064

18. Cohen-Kashi Malina K, Cooper I, Teichberg VI. Closing the gap between the *in-vivo* and *in-vitro* blood-brain barrier tightness. Brain Res. (2009);1284:12-21. https://doi.org/10.1016/j.brainres.2009.05.072

19. Haydon PG, Carmignoto G. Astrocyte control of synaptic transmission and neurovascular coupling. Physiol Rev. (2006);86(3):1009-31. https://doi.org/10.1152/physrev.00049.2005

20. Salmina AB. Neuron-glia interactions as therapeutic targets in neurodegeneration. J Alzheimers Dis. (2009);16(3):485-502. https://doi.org/10.3233/JAD-2009-0988

21. Koehler RC, Roman RJ, Harder DR. Astrocytes and the regulation of cerebral blood flow. Trends Neurosci. (2009);32(3):160-9. https://doi.org/10.1016/j.tins.2008.11.005

22. Krueger M, Bechmann I. CNS pericytes: concepts, misconceptions, and a way out. Glia. (2010);58(1):1-10. https://doi.org/10.1002/glia.20898

23. Alarcon-Martinez L, Yemisci M, Dalkara T. Pericyte morphology and function. Histol Histopathol. (2021);36(6):633-643. https://doi.org/10.14670/HH-18-314

24. Bonkowski D, Katyshev V, Balabanov RD, Borisov A, Dore-Duffy P. The CNS microvascular pericyte: pericyte-astrocyte crosstalk in the regulation of tissue survival. Fluids Barriers CNS. (2011);8(1):8. https://doi.org/10.1186/2045-8118-8-8

25. Dore-Duffy P, Katychev A, Wang X, Van Buren E. CNS microvascular pericytes exhibit multipotential stem cell activity. J Cereb Blood Flow Metab. (2006);26(5):613-24. https://doi.org/10.1038/sj.jcbfm.9600272

26. Peppiatt CM, Howarth C, Mobbs P, Attwell D. Bidirectional control of CNS capillary diameter by pericytes. Nature. (2006);443(7112):700-4. https://doi.org/10.1038/nature05193

27. Muoio V, Persson PB, Sendeski MM. The neurovascular unit - concept review. Acta Physiol (Oxf). (2014);210(4):790-8. https://doi.org/10.1111/apha.12250

28. Armulik A, Genové G, Mäe M, Nisancioglu MH, Wallgard E, Niaudet C, He L, Norlin J, Lindblom P, Strittmatter K, Johansson BR, Betsholtz C. Pericytes regulate the blood-brain barrier. Nature. (2010);468(7323):557-61. https://doi.org/10.1038/nature09522

29. Bouchard BA, Shatos MA, Tracy PB. Human brain pericytes differentially regulate expression of procoagulant enzyme complexes comprising the extrinsic pathway of blood coagulation. Arterioscler Thromb Vasc Biol. (1997);17(1):1-9. https://doi.org/10.1161/01.atv.17.1.1

30. Kim JA, Tran ND, Li Z, Yang F, Zhou W, Fisher MJ. Brain endothelial hemostasis regulation by pericytes. J Cereb Blood Flow Metab. (2006);26(2):209-17. https://doi.org/10.1038/sj.jcbfm.9600181

31. Kim SU, de Vellis J. Microglia in health and disease. J Neurosci Res. (2005);81(3):302-13. https://doi.org/10.1002/jnr.20562

32. Nayak D, Roth TL, McGavern DB. Microglia development and function. Annu Rev Immunol. (2014);32:367-402. https://doi.org/10.1146/annurev-immunol-032713-120240

33. Colonna M, Butovsky O. Microglia Function in the Central Nervous System During Health and Neurodegeneration. Annu Rev Immunol. (2017);35:441-468. https://doi.org/10.1146/annurev-immunol-051116-052358

34. Rodríguez-Gómez JA, Kavanagh E, Engskog-Vlachos P, Engskog MKR, Herrera AJ, Espinosa-Oliva AM, Joseph B, Hajji N, Venero JL, Burguillos MA. Microglia: Agents of the CNS Pro-Inflammatory Response. Cells. (2020);9(7):1717. https://doi.org/10.3390/cells9071717

35. Ronaldson PT, Davis TP. Regulation of blood-brain barrier integrity by microglia in health and disease: A therapeutic opportunity. J Cereb Blood Flow Metab. (2020);40(1_suppl):S6-S24. https://doi.org/10.1177/0271678X20951995

36. Bernier LP, Bohlen CJ, York EM, Choi HB, Kamyabi A, Dissing-Olesen L, Hefendehl JK, Collins HY, Stevens B, Barres BA, MacVicar BA. Nanoscale Surveillance of the Brain by Microglia via cAMP-Regulated Filopodia. Cell Rep. (2019);27(10):2895-2908.e4. https://doi.org/10.1016/j.celrep.2019.05.010

37. Mosser CA, Baptista S, Arnoux I, Audinat E. Microglia in CNS development: Shaping the brain for the future. Prog Neurobiol. (2017);149-150:1-20. https://doi.org/10.1016/j.pneurobio.2017.01.002

38. Liu LR, Liu JC, Bao JS, Bai QQ, Wang GQ. Interaction of Microglia and Astrocytes in the Neurovascular Unit. Front Immunol. (2020);11:1024. https://doi.org/10.3389/fimmu.2020.01024

39. Kaur IP, Bhandari R, Bhandari S, Kakkar V. Potential of solid lipid nanoparticles in brain targeting. J Control Release. (2008);127(2):97-109. https://doi.org/10.1016/j.jconrel.2007.12.018

40. Witt KA, Gillespie TJ, Huber JD, Egleton RD, Davis TP. Peptide drug modifications to enhance bioavailability and blood-brain barrier permeability. Peptides. (2001);22(12):2329-2343. https://doi:10.1016/s0196-9781(01)00537-x

41. Pardridge WM. Blood-brain barrier delivery. Drug Discov Today. (2007);12(1-2):54-61. https://doi.org/10.1016/j.drudis.2006.10.013

42. Pardridge WM. Molecular Trojan horses for blood-brain barrier drug delivery. Curr Opin Pharmacol. (2006);6(5):494-500. https://doi:10.1016/j.coph.2006.06.001

43. Gosselet F, Loiola RA, Roig A, Rosell A, Culot M. Central nervous system delivery of molecules across the blood-brain barrier. Neurochem Int. (2021);144:104952. https://doi: 10.1016/j.neuint.2020.104952.

44. Lipinski CA, Lombardo F, Dominy BW, Feeney PJ. Experimental and computational approaches to estimate solubility and permeability in drug discovery and development settings. Adv Drug Deliv Rev. (2001);46(1-3):3-26. https://doi:10.1016/s0169-409x(00)00129-0

45. Roskoski R Jr. Rule of five violations among the FDA-approved small molecule protein kinase inhibitors. Pharmacol Res. (2023);191:106774. https://doi:10.1016/j.phrs.2023.106774

46. Murugesan A, Konda Mani S, Koochakkhani S, et al. Design, synthesis and anticancer evaluation of novel arylhydrazones of active methylene compounds. Int J Biol Macromol. (2024);254(Pt 3):127909. https://doi:10.1016/j.ijbiomac.2023.127909

47. Huwyler J, Wu D, Pardridge WM. Brain drug delivery of small molecules using immunoliposomes. Proc Natl Acad Sci U S A. (1996) Nov 26;93(24):14164-9. https://doi.org/10.1073/pnas.93.24.14164

48. Chen TC, Wang W, Schönthal AH. From the groin to the brain: a transfemoral path to blood-brain barrier opening. Oncotarget. (2023);14:413-416. https://doi.org/10.18632/oncotarget.28414

49. Sánchez-Dengra B, González-Álvarez I, Bermejo M, González-Álvarez M. Access to the CNS: Strategies to overcome the BBB. Int J Pharm. (2023);636:122759. https://doi: 10.1016/j.ijpharm.2023.122759

50. Fong H, Zhou B, Feng H, Luo C, Bai B, Zhang J, Wang Y. Recapitulation of Structure-Function-Regulation of Blood-Brain Barrier under (Patho)Physiological Conditions. Cells. (2024);13(3):260. https://doi.org/10.3390/cells13030260

51. Virtanen PS, Ortiz KJ, Patel A, Blocher WA 3rd, Richardson AM. Blood-Brain Barrier Disruption for the Treatment of Primary Brain Tumors: Advances in the Past Half-Decade. Curr Oncol Rep. (2024);26(3):236-249. https://doi.org/10.1007/s11912-024-01497-7

52. Wang M, Etu J, Joshi S. Enhanced disruption of the blood brain barrier by intracarotid mannitol injection during transient cerebral hypoperfusion in rabbits. J Neurosurg Anesthesiol. (2007);19(4):249-56. https://doi.org/10.1097/ANA.0b013e3181453851

53. Hasegawa Y, Iuchi T, Sakaida T, Yokoi S, Kawasaki K. The influence of carmustine wafer implantation on tumor bed cysts and peritumoral brain edema. J Clin Neurosci. (2016);31:67-71. https://doi.org/10.1016/j.jocn.2015.12.033

54. Liu HL, Hua MY, Chen PY, Chu PC, Pan CH, Yang HW, Huang CY, Wang JJ, Yen TC, Wei KC. Blood-brain barrier disruption with focused ultrasound enhances delivery of chemotherapeutic drugs for glioblastoma treatment. Radiology. (2010);255(2):415-25. https://doi.org/10.1148/radiol.10090699

55. Gernert M, Feja M. Bypassing the Blood-Brain Barrier: Direct Intracranial Drug Delivery in Epilepsies. Pharmaceutics. (2020);12(12):1134. https://doi:10.3390/pharmaceutics12121134

56. Sousa F, Dhaliwal HK, Gattacceca F, Sarmento B, Amiji MM. Enhanced anti-angiogenic effects of bevacizumab in glioblastoma treatment upon intranasal administration in polymeric nanoparticles. J Control Release. (2019);309:37-47. https://doi:10.1016/j.jconrel.2019.07.033

57. Ferreira NN, de Oliveira Junior E, Granja S, Boni FI, Ferreira LMB, Cury BSF, Santos LCR, Reis RM, Lima EM, Baltazar F, Gremião MPD. Nose-to-brain co-delivery of drugs for glioblastoma treatment using nanostructured system. Int J Pharm. (2021);603:120714. https://doi:10.1016/j.ijpharm.2021.120714